nature reviews earth & environment

https://doi.org/10.1038/s43017-024-00584-4

Review article

Check for updates

Past climate change effects on human evolution

Axel Timmermann[1,2] ✉, Pasquale Raia[3] ✉, Alessandro Mondanaro[4], Christoph P. E. Zollikofer[1], Marcia Ponce de León[1], Elke Zeller[1,2] & Kyung-Sook Yun[1,2]

Abstract

The genus *Homo* evolved during the Pleistocene — an epoch of gradual cooling and amplification of glacial cycles. The changing climates influenced early human survival, adaptation and evolution in complex ways. In this Review, we present current knowledge about the effects of past climate changes on the evolutionary trajectory of human species. Humans emerged in dry grassland and shrubland when average climate conditions were warm. As global climate started cooling down, human species needed either to track their preferred habitats or to adapt to new local conditions, each of which is indicated in the archaeological record. Limited dispersal ability and narrow ecological preferences were predominant in early species, whereas cultural innovations and consequently wider ecological niches became commonplace in later species, allowing them to live in colder extratropical climates. Yet, despite their growing ecological versatility, all species but one eventually went extinct. Future research should explore cultural transmission between and within species, and the influence of climate change on human genetic diversification.

Sections

[1]IBS Center for Climate Physics, Busan, South Korea. [2]Pusan National University, Busan, South Korea. [3]DiSTAR, Università di Napoli Federico II Monte Sant'Angelo, Naples, Italy. [4]DST, Università degli Studi di Firenze, Florence, Italy. ✉e-mail: axel@ibsclimate.org; pasquale.raia@unina.it

Introduction

From the Pleistocene epoch to the Holocene (between 2.58 million years ago, Ma, and 11.65 thousand years ago, ka), *Homo sapiens* and earlier representatives of the genus *Homo* were subject to repeated cooling and warming events[1] (Fig. 1), alternating wet or dry conditions[2], modified seasonality and major vegetation shifts[3]. These often intense and rapid climate changes influenced the course of human evolution, driving or affecting intercontinental dispersal events, speciation, extinction, and biological and cultural adaptation. These processes helped to shape *Homo* into one of the most successful mammalian genera so far, diversifying a single, average-brained, warm-adapted African ape species into several large-brained, cold-tolerant taxa, which dispersed over the Old World, managed fire, and invented culture, clothes and complex tools along the way[4–6]. *Homo sapiens* is now the only surviving species in a highly dynamic multispecies evolutionary story that lasted for at least 3 million years.

Understanding of these climate impacts on hominins, however, has been hampered by the spatial resolution and temporal continuity of the archaeological record. As such, evidence is often limited to punctuated observations of habitat preferences, vegetation types[7–9], diet[10] and resource availability — typically in unusually rich archaeological sites. Indeed, geochemical[11,12] and palynological proxies[13,14] indicate a preference for open and grassy habitats in early *Homo*[6], and the inclusion of more meat and protein-rich food in later *Homo* such as Neanderthals[15]. But these records are not able to provide full determination of hominin ecological niches and niche evolution of metapopulations, limiting the ability to infer the actual impact of climate change on the evolutionary history of *Homo*[16].

Climate models now offer such an opportunity. Increasing computational power has enabled transient palaeoclimate simulations with coupled atmosphere–ocean models[17–19], filling the large temporal and spatial gaps in the palaeoclimate record. Accordingly, climate models have allowed explicit quantification of links between past climate change and human dispersal[20,21], habitat preferences[4,21], selection[3], adaptation, genetic admixture[22] and diversification[23], speciation and extinction[24,25]. Alongside developments in palaeobiology, palaeogenomics and ecological modelling, previously unexplored facets of *Homo* evolution have been illuminated. For instance, isotopic analyses of dental enamel help in understanding the diet of past human species[10,15], and modelling of their climate niche[24] indicates exposure to extinction risk. These approaches stem from geochemical, palaeoecological and even biological conservation research, rather than classic anthropology. Although changes in society and technology limit the value of such knowledge with regards to future human evolution (that is, as an analogue), the building and development of quantitative modelling tools do enable insight into past, present and future responses to environmental challenges.

In this Review, we discuss how climate and vegetation shifts were important drivers of hominin evolution, focusing on areas covered by extensive modelling and anthropological research — namely Pleistocene Africa and Eurasia. We begin by describing the mathematical frameworks that can be used to conceptualize key processes in hominin evolution or make quantitative assessments. We follow by discussing major palaeoclimate and ecosystem changes, before outlining how these changes influenced human evolutionary history, including speciation, niche occupation, extinctions and cultural innovation. We end by outlining future research priorities, arguing the need to further address the role of climate in cultural adaptation and genetic diversification.

Modelling human responses to climate

Spatially and temporally resolved multidimensional palaeoclimate datasets[26] enable inferences on the ecological niche of hominins beyond those derived from single point observations at individual sites. Realistic spatiotemporal environmental data can be used to identify and simulate preferred human habitats and dispersal behaviours, among other aspects of hominin evolution.

Species distribution models

Species distribution models (SDMs) are a powerful biogeographical statistical modelling tool to link extant or past species occurrences with environmental variables in terms of time-invariant statistical relationships. Using spatial and temporal environmental inputs, SDMs can predict the habitat suitability of a species, which is a measure of the overlap between the species-specific climate envelope and the actual climate conditions. By combining palaeoclimate and environmental data with fossil and/or archaeological datasets of hominin presence[21,24] and absence, SDMs can help to test hypotheses about the climate preferences of ancient hominins.

An SDM is a function $H(C_i, \ldots C_{N_c})$ that characterizes the occurrence probability of a species in relation to climate or environmental variables $C_i (i = 1, \ldots N_c)$. SDMs are derived from empirical presence or absence data for the species at different locations over all relevant sample ages and corresponding data or modelling estimates of environmental conditions. In this formulation, H, habitat suitability, is an implicit function that describes an estimate of the potential climate niche of a species. C_i typically depends on longitude, latitude (x, y) and time t, $H(C_i(x, y, t), \ldots C_{N_c}(x, y, t)) = H(x, y, t)$. Importantly, SDMs identify the realized niche of a species (the fraction of the fundamental niche currently exploited by the species), whereas the fundamental niche includes the full range of physiological tolerance limits and resource needs of that species. Palaeoclimate model simulations[5,26–33], or climate emulators[34–36] with gridded $[(x, y, t) \rightarrow (x_k, y_k, t_j)]$ estimates of the climate variables C_i, can then be used to obtain a time-evolving spatiotemporal environmental data vector $\mathrm{V} = [C_1(x_k, y_k, t_j), \ldots C_{N_c}(x_k, y_k, t_j)]$. The temporal evolution of the habitat suitability can be calculated as $H(x_k, y_k, t_j) = H(\mathrm{V})$. Selection of multidimensional climate variables to estimate an SDM depends on the specific application. For example, different combinations of variables characterizing temperature and water tolerances, or human food resources (net primary productivity), can test different hypotheses about the factors influencing human distributions[21,22,37,38]. Reducing dimensionality in the input variables is essential to avoid overfitting SDMs owing to strong statistical codependencies[39–41].

SDM algorithms differ in how they model the species niche. Machine learning approaches (Maxent[42], Random Forest[43]) or ecological niche factor analysis[44] are best used in data-rich situations, when more than 50 discrete observations (species presence datapoints) from different geographical locations are available. Other SDMs use drivers of species distribution other than climate conditions, such as intrinsic physiological tolerances (mechanistic models[45]); or use patterns of species co-occurrence[46] or phylogeny[47]; or combine co-occurrence with climate data[48], and mechanistic models with presence-only (climate envelope) models[49]. Presence or absence data generally provide a better delineation of the species niche than presence-only data[50]. When working with scarce presence data[51,52], such as for extinct hominins, or when applying SDMs to non-analogous climate situations[47,53], the best approximation of the fundamental niche[54,55] can be obtained by supplementing observational data with phylogenetic information[22,24,47,56].

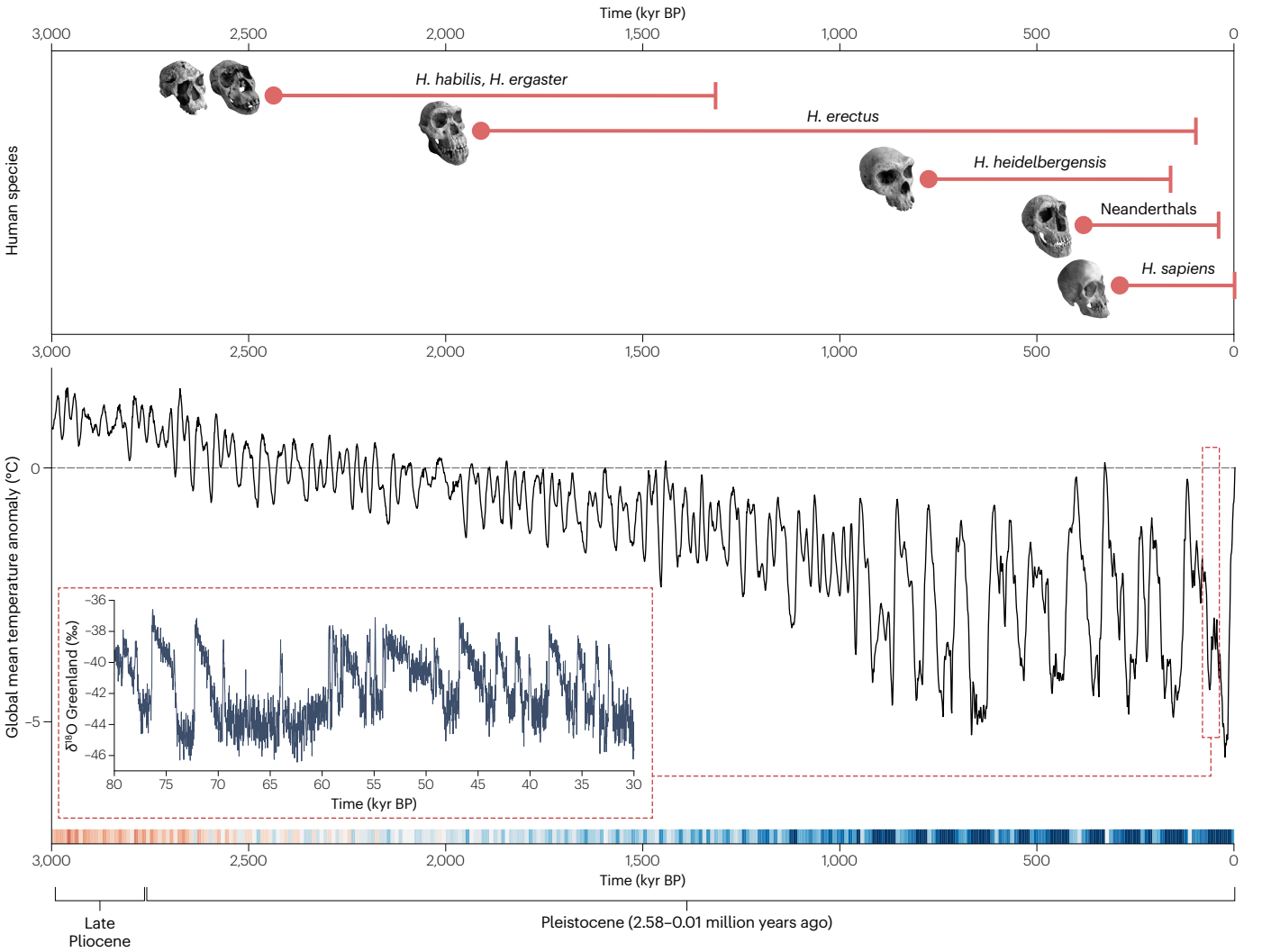

Fig. 1 | Palaeoclimate and human evolution timeline. Upper part: estimated age range for human species (red lines; *Homo habilis*, *H. ergaster*, *H. erectus*, *H. heidelbergensis*, *H. neanderthalensis* and *H. sapiens*), and their representative skull specimens. Lower part: modelled global mean temperature anomaly (black line) and corresponding warming stripes (red–blue stripe) from the Late Pliocene to the Holocene epoch (3,000–0 kyr BP), relative to preindustrial; model data are from a transient CESM1.2 simulation[18,21] run with orbital forcing and estimates[26] of ice-sheet extent and CO_2. Inset: oxygen isotope data ($\delta^{18}O$) from Greenland ice cores[192] over 80–30 kyr BP. During their evolution, human species were exposed to large-scale climate reorganizations on millennial to orbital timescales.

Density-based models

Density-based modelling is another approach used to infer how climate influenced the abundance of human species and other characteristics through time. Partial differential equations are used to predict species densities as a function of time and space. In contrast to species distribution models, this approach does not rely on extensive empirical datasets of fossils or archaeological artefacts, but rather on parameters characterizing human reproductive rates, mortality and mobility.

Groups of individuals of the same species and with the same environmental tolerances can be described by a continuous population density variable[57] ρ, which depends on longitude and latitude (x, y) and time t. This approach recognizes populations as quasi-continua, which can disperse through diffusive or advective[58,59] processes, grow in the presence of sufficient food resources (typically described through a carrying capacity K) or decline when population density exceeds the carrying capacity[60]. The combined dispersal and growth dynamics of a population are typically modelled with the Fisher–Kolmogorov–Petrovsky–Piskunov (F–KPP) reaction–diffusion equation[57]:

$$\frac{\partial \rho}{\partial t} = \nabla(\kappa \nabla \rho) + \alpha \rho\left(1 - \frac{\rho}{K}\right). \quad (1)$$

The left side of the equation denotes the temporal change of population density ρ. The first term on the right side denotes diffusion (in which κ represents the diffusivity) and the second term denotes density-dependent growth with an intrinsic population growth rate α. The carrying capacity K determines how many individuals per unit area

can be maintained by the existing climate-dependent food resources in equilibrium. If $\rho > K$, and in the absence of dispersal, the logistic term becomes negative, and the population begins to decline. If a population moves into an unoccupied[61] region, the minimum propagation speed of the population front according to equation (1) can be obtained from the Fisher travelling wave equation[57,62] as $v = 2\sqrt{\alpha\kappa}$. Habitat tracking (the ability of a species to disperse toward suitable habitats when local conditions deteriorate) is possible when the propagation speed v is equal to or larger than the magnitude of the climate-induced habitat velocity. This relationship can be expressed as $V_{cl} = \frac{dK}{dt}(\nabla K)^{-1}$, in which the first term represents the temporal change in carrying capacity and the second term the spatial gradient. V_{cl} represents the speed at which areas with similar carrying capacity shift their geographical location. If $\frac{dK}{dt} < 0$ (that is, if local habitat conditions or food resources deteriorate, for example owing to a long-term drought), habitat tracking of hominins is likely to occur in the direction of a positive habitat gradient, which means that humans would be moving towards wetter conditions with more available food resources. Under deteriorating local conditions, $v < |V_{cl}|$ can cause environmental stress to accumulate, acting as a driver for regional adaptation or regional extinction. The key parameters K, α and κ in equation (1) can be estimated empirically, for instance from present-day hunter-gatherer groups[57,61]. F–KPP models have become powerful explanatory tools to interpret archaeological data, human migration, and the emergence of new populations and traits in remote regions[57,63–65].

The carrying capacity K in these models represents the climate forcing of the dynamical population model obtained from palaeoclimate model simulations. Instead of the common assumption that K is only related to the available net primary production[5,20,23,66] $\mathrm{NPP}(x, y, t)$, the NPP can be additionally weighed by the species' habitat suitability $H(x, y, t)$, thereby combining density-based models (equation (1)) with SDMs. The carrying capacity K can then be expressed as $K(x, y, t) = \eta \mathrm{NPP}(x, y, t)H(x, y, t)$. Another possibility to account for species-specific food and climate preferences is to include the habitat weighting $H(x, y, t)$, in the net growth parameter α. These formulations require the prior computation of habitat suitability maps for different time periods using archaeological and/or anthropological and climate data.

Agent-based models

Agent-based models (ABMs) use algorithmic rules to specify the behaviour of discrete, mobile agents — individuals or groups of individuals — interacting with each other and their environment. These ABMs allow one to ask how small-scale or short-term processes and patterns of individual behaviour, movement and interaction with the environment give rise to the large-scale or long-term processes and patterns of human population dynamics in space and time. Weak-emergence[66,67] questions have long been at the core of agent-based modelling in archaeology and related fields[68–70]. Implementing an ABM requires decisions about which empirical data to use to design the model agents, and at what temporal and spatial resolution agents operate. The challenge is to balance the level of detail and realism of the agents with the available empirical data and the resulting computational costs.

To illustrate the value of ABMs for understanding hominin evolution, consider an example of a global ABM[20,71] to simulate human dispersals under late Pleistocene climate fluctuations. Its temporal resolution (in this case, one year) and geographical grid resolution essentially determine the level of detail of the agent implementation. The corresponding agents are female and male individuals that perform yearly actions such as 'move', 'mate', 'give birth', 'grow' and 'die', whereas daily actions such as 'forage', 'hunt', 'eat' and 'sleep' are not incorporated in the model. The probabilistic scheduling of the agents' yearly actions is based on empirical data on present-day hunter-gatherers, and on inferences drawn from archaeological evidence of past lifestyles. Climate-dependent food resources and limitations for the individual agents are parameterized through a carrying capacity term obtained from climate model simulations. Notably, the ABM does not explicitly implement macroscopic parameters used in F–KPP models (equation (1)) such as population growth rate α and population diffusivity κ. Rather, α and κ emerge as system properties from the combined effects of individual birth, growth, reproduction and death events, of individual movement bouts, and of the interactions of individuals with each other and with the environment.

The main advantage of ABMs over density-based models is that they represent the discreteness and heterogeneity of real-life individual processes and actions[20,72,73], such as the exchange and/or transmission of information among individuals. Individuals can propagate information via genetic pathways, or culturally by sharing skills. In principle, it is possible to simulate gene–culture coevolution and genetic–cultural adaptation under fluctuating climate conditions[23] using complex model agents with large parameter sets to quantify these properties. However, overparameterization critically limits the informative power of ABMs. The fewer parameters they use to model individual agents, the better they express our limited knowledge of fossil human individuals and the greater their explanatory power. Such considerations are of critical relevance for modelling the late Pleistocene dispersals of human populations from Africa and their interactions with local Eurasian populations such as the Neanderthals and Denisovans.

Palaeoclimate and ecosystem changes

Substantial climatological change occurred during the time since the evolution of the first *Homo* to the beginnings of a sedentary lifestyle of *Homo sapiens* (that is, from around 2.8 Ma to the beginning of the Holocene, around 11.65 ka; Fig. 1). In this section, the major changes to physical climate and their cascading effects on the evolution of ecosystems are described.

Physical climate

Glacial cycles, the waxing and waning of major ice sheets, are a key component of palaeoclimate variability, determined in large part by astronomical forcings called Milanković cycles[74] (Fig. 2). These forcings, which influence climate variability on timescales of 20–400 thousand years (kyr) (Fig. 1), reflect changes in Earth's axis tilt (obliquity), the shape of Earth's orbit around the Sun (eccentricity) and Earth's axis wobble (precession). Milanković cycles cause shifts in the seasonal distribution of solar radiation, which can in turn generate temperature gradients and corresponding shifts in atmospheric circulation and precipitation[75]. When the precession index is negative, Earth is closer to the Sun in boreal summer, which leads to Northern Hemisphere summer warming and related northward shifts in tropical rainbands[76–81]. These dynamics are evident in monsoon systems and the extensive intertropical convergence zones — zonally extended bands of increased rainfall and weak winds, and important energy sources for the atmospheric circulation[82]. Precessional shifts of the intertropical convergence zones and monsoon systems cause regional wet–dry cycles which have been suggested as drivers of human evolutionary change in Africa[5,12] and Asia[83].

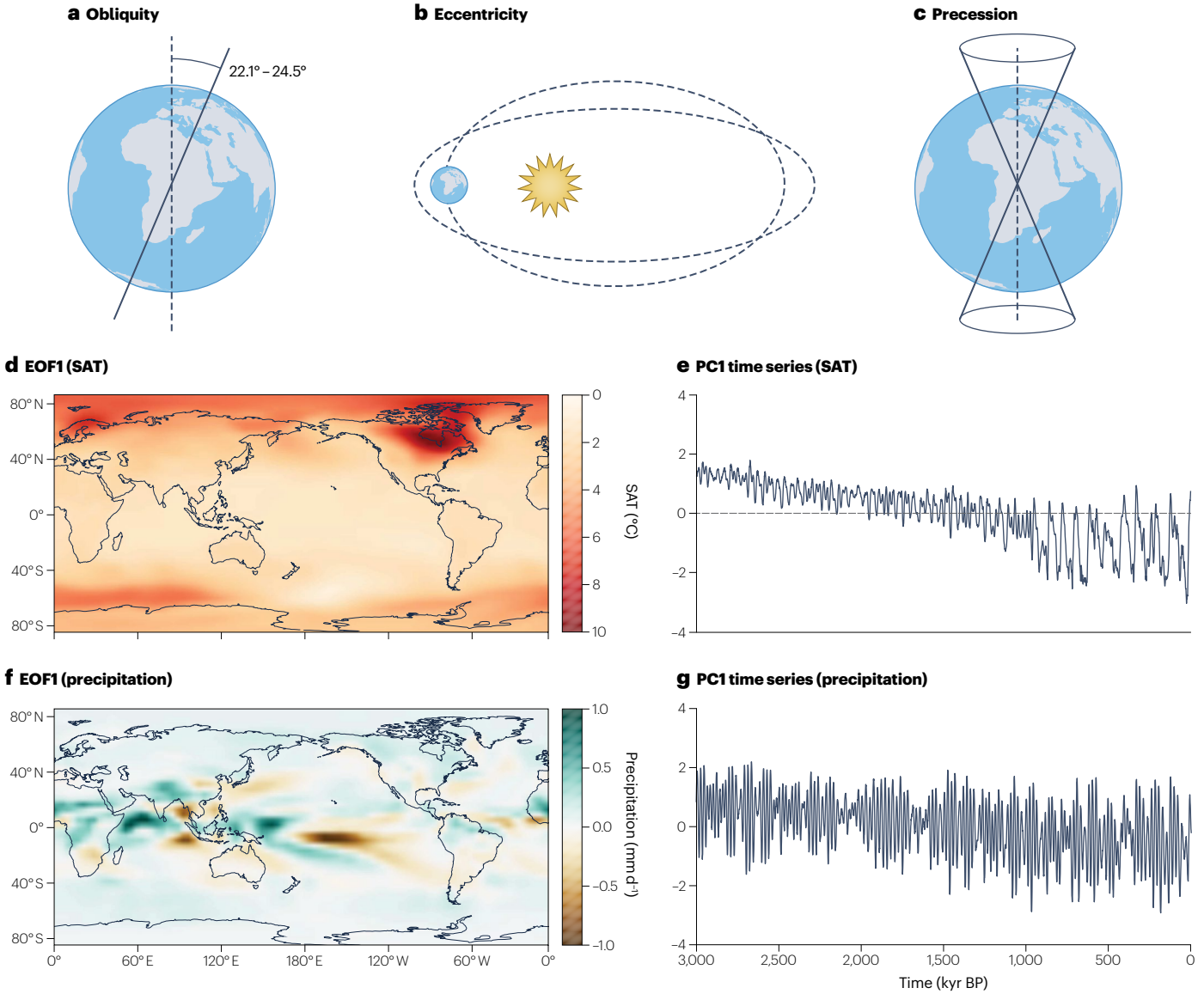

Fig. 2 | Climate response to astronomical forcings. a, The obliquity component of the Milanković cycles, reflecting changes in Earth's axial tilt. **b**, The eccentricity component of the Milanković cycles, reflecting changes from a circular to elliptical orbit of Earth around the Sun. **c**, The precession component of the Milanković cycles, representing axial and apsidal precession. **d**, The leading empirical orthogonal function (EOF) of simulated[21] surface air temperature (SAT) over the past 3 million years. **e**, The corresponding principal component (PC) time series for panel **d**. **f**, As in panel **d**, but for precipitation. **g**, As in panel **e**, but for precipitation. Milanković cycles served as the metronome of climate change during the Pleistocene, creating glacial–interglacial cycles and massive shifts in tropical rainfall.

Temperature and precipitation are the main aspects of spatiotemporal climate variability that are likely to have affected hominin groups[4,12,84,85] (Fig. 2d–g). Throughout the Pleistocene, Earth's climate gradually cooled and the amplitude and duration of major cold–warm (glacial–interglacial) transitions increased. The Mid-Pleistocene Transition[86] (MPT) occurred around 1,000–800 kyr before present, when the dominant ice-age cyclicity switched from 20–40 kyr to 80–120 kyr. After the MPT, glacial periods characterized by global cooling of up to 5 °C (relative to late Holocene conditions, Fig. 1) became dominant, interrupted by interglacial episodes typically lasting for 10–20 kyr. To understand human responses to this variability, it is important also to document the regional aspects of palaeoclimate change. The leading mode of surface temperature variability simulated by a climate model[18] is characterized by a homogenous warming pattern (Fig. 2d). The amplitude of this pattern, however, decreased gradually over the past 3 million years (Fig. 2e), in agreement with the global mean cooling trend (Fig. 1) driven by decreasing atmospheric CO_2 concentrations[26]. Superimposed on the cooling trend is variability in the form of warm–cold fluctuations, caused by glacial–interglacial CO_2 variability and the orbital-scale waxing and waning of ice sheets, affecting mainly northern North America and Scandinavia.

Pleistocene precipitation variations are best described by a highly complex and heterogenous dominant tropical pattern of variability[76] (Fig. 2f), showing shifts in the major tropical rainbands. These trends in turn affected vegetation patterns and environmental conditions relevant to early hominin evolution and dispersal[5]. The temporal change of the leading mode of precipitation variability is characterized by strong eccentricity-modulated precessional cycles and an overall declining trend (Fig. 2g).

In addition to these astronomically forced climate changes, the Pleistocene was also punctuated by millennial-scale transitions, known as Dansgaard–Oeschger (DO) cycles[87,88], that caused massive shifts in hydroclimate and vegetation[89,90]. DO events, which were more prevalent for medium-sized ice sheets[91], are typically characterized by relatively fast warming from cold (stadial) to warm (interstadial) conditions in the Northern Hemisphere, followed by a gradual cooling[92] (Fig. 1, inset). The Southern Hemisphere exhibited an out-of-phase relationship known as the bipolar seesaw[29,93]. DO events lacked clear periodicity, and their return time ranges from decades (DO precursor events) to millennia. DO variability can be generated by internal ocean–climate instabilities[94–99], often related to the so-called deep-decoupling oscillations[100,101], or by ice-sheet instabilities and corresponding freshwater input originating from the Eurasian[102,103] or the Laurentide ice sheets, or both[29].

Together, orbital, millennial-scale and shorter-term changes in climate influenced vegetation and ecosystems where early humans evolved.

Biome changes

The variety of habitats shared by large species communities can be summarized in terms of biomes. A biome is typically characterized by a distinctive plant community, which is in turn determined by specific conditions in the physical environment. Thus, modelling past climate variability and change provides an opportunity to infer changes in the regional distribution of biomes through time. This taxon-free approach seeks to model the past biomes rather than their constituent species. To identify ecosystem preferences of early human species, it is appropriate to first assess the more robust comprehensive megabiomes, namely tropical forest, temperate and boreal forests, grassland–dry-shrubland, savanna–dry-woodland, desert and tundra[104] (Fig. 3).

Simulations of global vegetation[3] indicate that global cooling during the Pleistocene and shifts in precipitation patterns caused major shifts in the dominant megabiome types (Fig. 3). After the MPT, persistent early Pleistocene temperate forest in Europe was replaced by intermittent episodes of temperate and boreal forest, occurring mostly during interglacial periods (Fig. 3c). Glacial periods in Europe were characterized by an extensive coverage of grassland, dry shrubland and tundra, and a substantial reduction in forested areas.

Over Asia and equatorward of 45° N, model simulations[3] yield rather stable environments, which were only punctuated by precessional-scale variability with a period of about 21 kyr (Figs. 2c,3). At high latitudes, glacial tundra alternated with boreal forests on timescales of 20–40 kyr prior to the MPT and 80–120 kyr subsequently. In Central Africa, biomes shifted from rainforests to more open environments (grassland and shrubland) after the MPT. In northern Africa, vegetation variability was characterized by strong precessional cycles, which might have played a major role in creating green corridors[4,5,12,85,105] between northern Africa, the Levant and the Arabian Peninsula.

Climate effects on human evolution

Changes in climate influence the amount and type of resources[106], and the location, size and degree of connection between the habitable places available to species[55,107,108]. For most species, the main biological response to climate change is habitat tracking — that is, the tendency to follow their preferred habitats as climate disturbances push them towards different areas[109], even on seasonal timescales. Because habitat tracking is a species' response to climate change without adaptation, it is thought to be the main determinant of evolutionary stasis[110,111]. However, habitat tracking is just one possible response to climate change and requires species to be mobile enough to keep track with the climate-induced habitat velocity V_{cl} (Fig. 4b). Other responses to climate change include adaptation and extinction (that is, the lack of an effective response; Fig. 4a). This section describes a selection of illustrative key examples that document how modelling approaches can be used to test hypotheses about evolutionary responses to past climate change.

The expanding human niche

During the Pleistocene, hominin species expanded several times from Africa into Eurasia (Fig. 5a), requiring adaptation to new environmental conditions beyond subtropical and extratropical biomes, such as temperate and boreal forests. Using an extensive critically assessed dataset of locations and ages and age uncertainties of different hominin species[21,24] (Fig. 3) in combination with a transient global biome simulation (Fig. 3a–c), the proportion of biomes inhabited by the different hominin groups can be determined. Accordingly, early African hominins (*H. ergaster*, Fig. 5b) were more specialized than later *Homo* species and preferred open environments — mostly grass and shrubland and to a lesser extent savanna. As *H. erectus* populations dispersed into Eurasia roughly 2 Ma (Fig. 5a), they adapted to temperate and tropical forests, but showed little tolerance for colder extratropical conditions in boreal forest biomes (Fig. 5c). The peopling of Europe by *H. erectus* might not have been continuous but rather interrupted by an abrupt climate change event ~1.126 Ma (ref. 1) corresponding to marine isotope stage (MIS) 34, suggesting that this species did not have sufficient cultural tools to withstand the new cold conditions (Fig. 5a).

Homo heidelbergensis first encountered the intensifying amplitude of post-MPT glacial–interglacial cycles when they dispersed into Eurasia (Fig. 5a) around 800–600 ka. The Eurasian populations were able to survive this climate variability by expanding their biome niche into boreal forests. The climate and biome niches of *H. neanderthalensis* were similar to those of *H. heidelbergensis*, thus supporting the notion of close phylogenetic relationships[21] (Fig. 5a,d,e). Apart from the dominant temperate forest and grass and/or shrubland habitats, which were often found during glacial periods in the Mediterranean region (Fig. 3c), Neanderthals were also able to adapt to colder climates characterized by tundra — but, surprisingly, to a lesser degree than typically assumed[3] (Fig. 5e). Eventually, *H. sapiens*, like no other species before, developed the skills to survive even in the harshest environments such as desert and tundra (Fig. 5f).

Environment, selection and adaptation

Various hypotheses have been proposed to explain how environmental factors might have shaped the speciation of hominins from the very emergence of the human clade. Among the early hypotheses is the savanna hypothesis[112] and more modern variants thereof[113], which posit that gradual cooling and drying of Africa (Fig. 2e,g) and the expansion of the savanna biome[114] (meant as a seasonal mosaic environment[113])

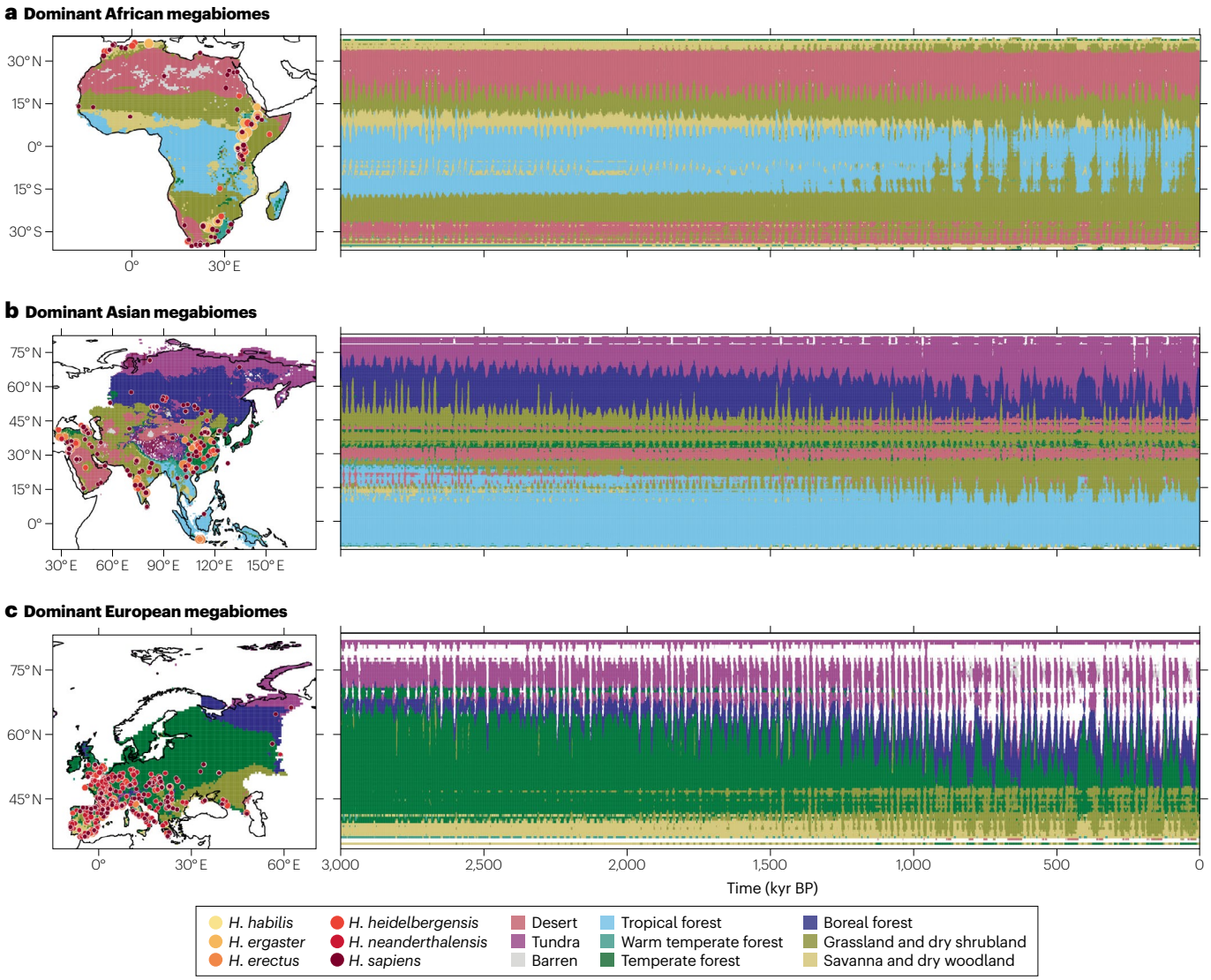

Fig. 3 | Past shifts in vegetation. a, African hominin sites (left, shaded circles), spatial distribution of dominant megabiomes over the past 3 million years (left, shading) and their latitudinally averaged temporal changes (right); data are from the BIOME4 model[193] forced with climate and CO_2 data from a CESM1.2 transient simulation[3,21]. **b**, As in panel **a**, but for Asia. **c**, As in panel **a**, but for Europe. Following the Mid-Pleistocene Transition (~0.9 Ma), the variability in vegetation types increased, and an overall trend towards colder biomes emerged.

contributed to the development of bipedalism and other marked features of early hominins. The savanna hypothesis stems from the notion that bipedal posture and movement offered advantages in seeking resources in open, savanna-like environments relative to forested habitats. These models have been challenged by fossil evidence[115], which shows an adaptation of early Hominidae (*Australopithecus*) to woodlands, rather than savanna, as well as by biome simulations which show wide expanses of tropical forest in central Africa along with grass and shrubland during the Pliocene[116] and Late Pliocene[3], but relatively limited regions present with actual savanna biomes (Fig. 3a). Nonetheless, the preference of early Pleistocene African *Homo* (such as *H. ergaster*) for open environments – primarily grass and shrubland – is still evident (Fig. 5b).

Other hypotheses of hominin speciation mechanisms emphasize the role of Milanković-scale climate variability (Fig. 1a-c). The variability selection hypothesis[117,118] and the pulsed climate variability hypothesis[2] propose that wet–dry cycles in Africa with alternating amplitudes contributed to adaptation, to speciation and possibly also to the increasing complexity and positive trend in relative brain volume, referred to as encephalization. At the core of this idea is that large environmental stress associated with increased climate variability created adaptation pressure (Fig. 4a). Groups that adapted to periods of high stress, by developing new social skills, better tools and/or hunting techniques, were able to expand their climate niche and geographical range when the stress decreased. The pulsing in stress and climate velocity has previously been associated with the 80–120 and 405-kyr eccentricity

cycles that modulated the precessional effect on rainfall, and eventually climate stress in central Africa[21] (Fig. 4b). This selection for resilience to temporal climate variability and the broadening of the climate niche would have allowed rapid colonization of new habitats during periods of climate stability (Fig. 4), as suggested by the accumulated plasticity hypothesis[119,120]. The accumulated climate-driven adaptation and niche expansion in African early *Homo* species might have eventually contributed to the ability of *H. erectus* to colonize Eurasia (Fig. 5c). In contrast, later human species (such as *H. heidelbergensis*) with a broader climate niche and improved technological innovations (mastering fire, using caves for shelter, production of fitted clothing) had a reduced need to adapt to time-varying climate stress. This enabled them to disperse more easily across continents, climate zones and biomes.

Ecosystem diversity in general, and spatial biome diversity in particular, had a fundamental role in expanding the large-scale human climate niche[3]. According to this continental-scale diversity selection hypothesis[3], which was derived empirically from a compilation of fossil and archaeological data and a vegetation model simulation, Late Pleistocene human populations were adapted to environments with greater regional diversity of plant and animal resources; this diversity of resources might have contributed to their resilience to perturbations in climate. This hypothesis neither presupposes nor excludes the effect of fluctuating climate conditions but emphasizes that biodiversity hotspots might have provided advantageous conditions for human groups that were able to benefit from ecosystem diversity, compared with those that relied on more specialized food resources.

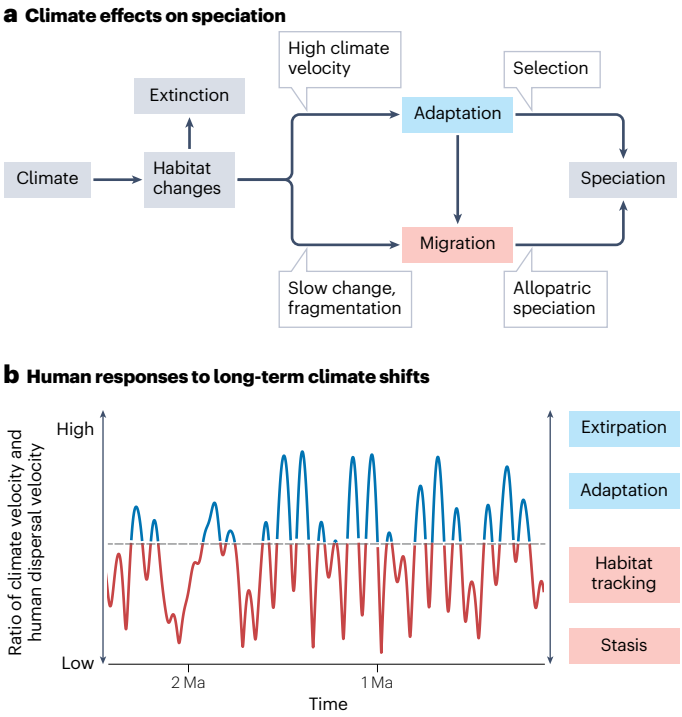

Fig. 4 | Climate impacts on human evolution. a, A schematic of the potential mechanisms by which climate pressures can induce or contribute towards speciation, adaptation and extinction. **b**, A time-series illustration of human responses to long-term climate fluctuations associated with the eccentricity cycle. The ratio between climate velocity and human dispersal velocity characterizes migration or adaptation trends in humans.

Migration and dispersal

During the early stages of its existence, the genus *Homo* was confined to Africa, where most speciation events within the genus occurred[121]. At least three major dispersal events outside the continent can be associated with different species (Fig. 5a). The first known long-distance dispersal is attributed to *H. erectus* entering Eurasia at least 1.8 million years ago[122], perhaps even as early as 2.48 Ma (ref. 123). The species eventually colonized most of the southern part of Asia, including as far east as Java[24,124]. The second event is attributed to *H. heidelbergensis*, which colonized as far north as England around 700 ka and possibly earlier[125], despite the onset of unprecedented cold conditions. Finally, *H. sapiens* colonized Eurasia (possibly through repeated dispersal waves) starting around 200 ka (refs. 126–129) and venturing into the Americas across glacial Beringia around 21 to 23 ka (ref. 130). There is some indication that human dispersal was limited by climate change[61] so that people migrated from less to more habitable places. However, climate change could also have favoured migration. The early colonization of Europe by *H. erectus* appears to have been triggered by the emergence of open vegetation and interglacial conditions[131], whereas warm and wet conditions likely facilitated the dispersal of *H. sapiens* out of Africa[4].

Early African hominins dispersed much faster than fellow primates, indicating that fast diffusion is a typical feature of the genus *Homo*[132]. Moving to the early Holocene, *H. sapiens* exhibited unparalleled dispersal ability with estimated dispersal rates of several hundreds to thousands of square kilometres per generation[57,64]. Early hunter-gatherer societies are deemed to have moved in the range of 1–10 km yr^{-1}, which echoes the velocity for the spread of farming indicated by reaction–diffusion modelling[65].

Key insights into human dispersals have come from reaction–diffusion and agent-based model simulations. An ensemble of climate-forced ABM simulations[71] indicated that *H. sapiens* dispersal events during MIS 3 and subsequently were limited to windows of opportunity around 55 ka and during the early to mid-Holocene (~9 ka). Both windows were associated with strong boreal summer insolation and the corresponding wet conditions in the Sinai region[21] (Fig. 6). Simulated populations of *H. sapiens* in Africa that failed to cross into Eurasia were unable to disperse until the next green corridor opened, offering new routes through the Sinai Peninsula into the Levant or across the Bab El Mandeb strait into the Arabian Peninsula. The subsequent evolution of these groups in Eurasia, as well as the interaction with other archaic hominin species (Neanderthals and Denisovans) would therefore have been partly affected by this astronomically paced climate gatekeeper (Fig. 2).

Extinctions

Central open questions in human evolutionary history ask which factors and processes governed the replacement of populations and the emergence and extinction of species. Four potential explanations have been discussed in relation to extinctions: climate fluctuations[1,24,107,133], differential population characteristics[25], assimilation and disease load[134]. The relative influences of these four factors on hominin extinctions have been explored using a variety of numerical models without and with spatial complexity.

Simulations of Neanderthal extinction in Eurasia with a realistic reaction–diffusion model[25] suggest that millennial-scale DO variability was not a dominant driver of extinction ~38–33 ka. A density-based dynamical model with and without this variability showed that the overall timing of Neanderthal extinction remained unaffected, although regional extirpations in high latitudes were more strongly affected by millennial-scale climate events. Simulations further indicated that

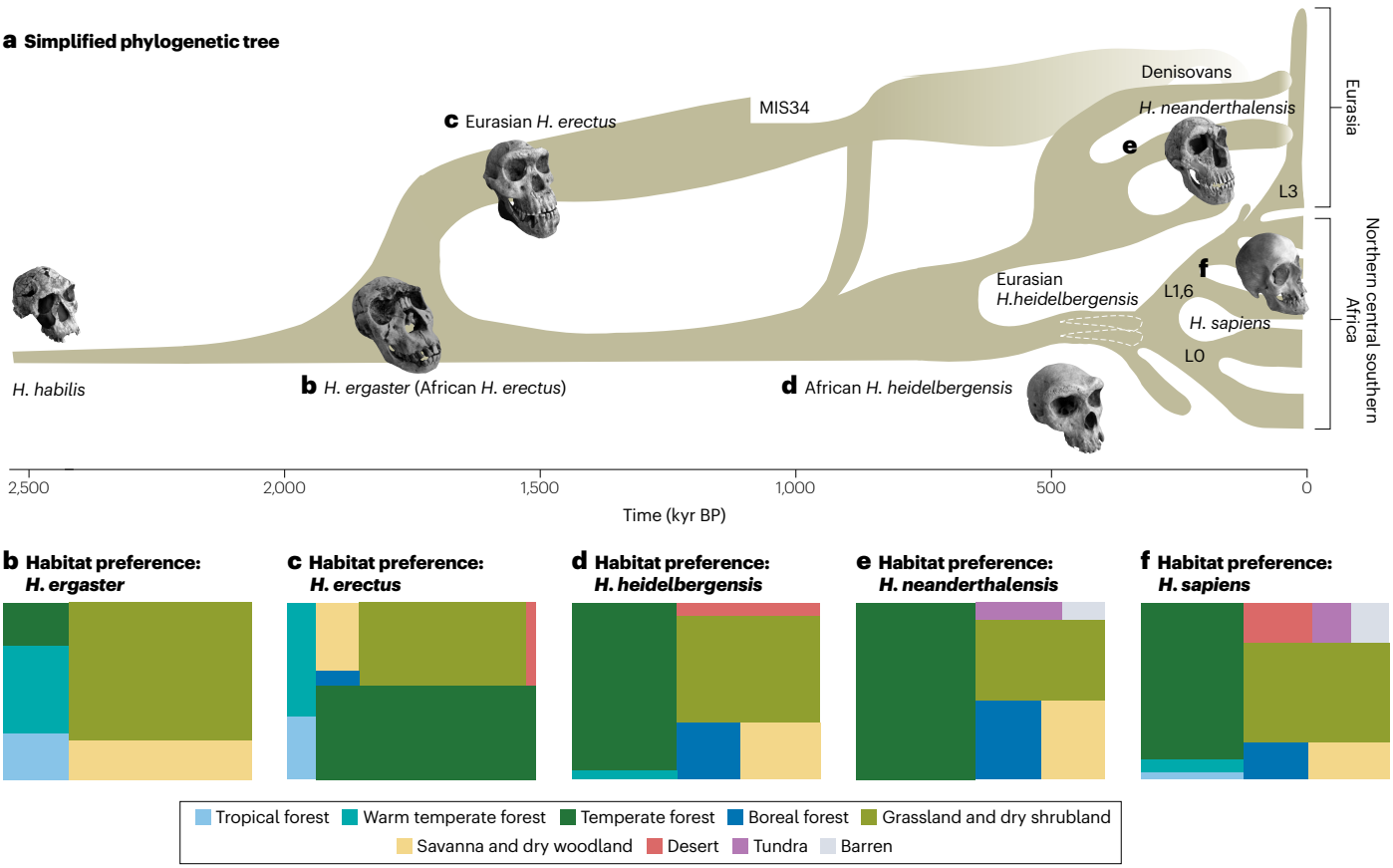

Fig. 5 | Human preferences for biomes. a, A simplified and hypothesized phylogenetic tree of seven hominins in the genus *Homo*, with the *Homo sapiens* branch stratified into different mitochondrial clades (L0, L1,6, L3) based on estimates of mitochondrial DNA coalescence times from extant populations[194,195]. **b**, Megabiome preferences for *H. ergaster*, obtained by extracting biome data from a 3 Myr transient simulation[3] for hominin sites and corresponding ages. **c**, As in panel **b**, but for *H. erectus*. **d**, As in panel **b**, but for *H. heidelbergensis*. **e**, As in panel **b**, but for *H. neanderthalensis*. **f**, As in panel **b**, but for *H. sapiens*. Hominins initially preferred open environments (grassland, dry shrubland and savanna), but expansion into Eurasia changed habitat preferences toward forested regions, with *H. sapiens* able to adapt to all megabiome types.

H. neanderthalensis populations collapsed around 48–38 ka, after *H. sapiens* dispersed from Africa through green corridors into Europe and outcompeted Neanderthals. Climate shifts might have also benefited Neanderthal survival, at least temporarily, by isolating the last Neanderthals living in southern Iberia from the incoming *H. sapiens* populations[135].

Using an ABM approach with a wide range of multiparameter simulations[20] (Fig. 6), a more refined regional and picture emerges, according to which only a small subset of climate and demographic parameter settings yielded a dispersal into Eurasia, as well as a complete extinction of archaic Eurasian populations, respectively. These simulations indicate competitive advantages of *H. sapiens* over archaic hominins, particularly the asymmetry in reproduction rates. The fact that climate-driven out-of-Africa dispersals preconditioned the subsequent species replacements and extinctions in Eurasia further supports the notion of precessional cycles in rainfall (Fig. 2) and net primary productivity (Fig. 6) influencing evolutionary processes.

Cultural adaptation

Cultural innovation and cumulative culture are hallmarks of the human lineage. Cultural innovations, such as mastering of fire and the invention of clothes and projectile weapons, allowed hominins to withstand climate challenges and to widen their resource base both locally and during their expansion into other continents and biome types outside their original climate niche (Fig. 5), rather than simply track habitats[56] (Fig. 7a).

Correlating the types and abundance of different cultural objects (such as tools and clothing) with climate conditions can suggest potential ways that climate and culture were interlinked[6,136]. For example, the onset of the MPT in the Nihewan Basin (China) seemingly coincided with increased diversity in tool production[137]. In the same region, strong climate oscillations during the Last Glacial Maximum coincided with waxing and waning usage of microblade technologies[138] by *H. sapiens*. A major change in African hydroclimate around 300 ka might have influenced the emergence of Middle Stone Age technology[139]. In South Africa, the emergence and disappearance of middle stone age innovations has been explained in terms of millennial-scale DO cycles, as exemplified by Still Bay and Howiesons Poort industries at around 71 and 64–59 ka, respectively[140,141]. In Western Europe, the advent of Acheulean technology (characterized by the production of hand axes) around 700 ka seems related to the dispersal of a new hominin species

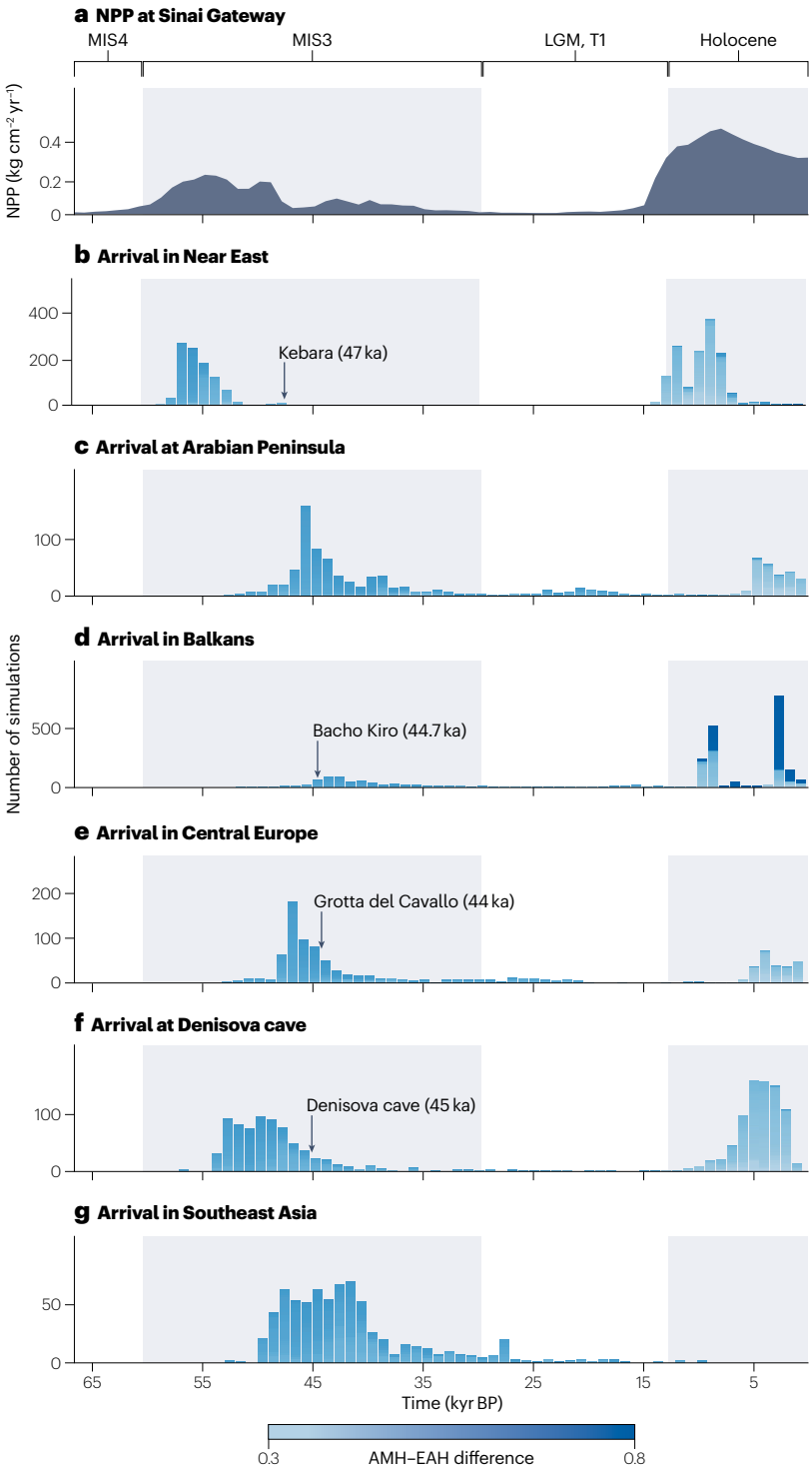

Fig. 6 | Dispersal of anatomically modern humans. a, Net primary productivity (NPP) at the Sinai Gateway over the past 65 kyr, taken from the LOVECLIM Earth System model[5]. **b**, The number of simulations indicating arrival of *Homo sapiens* in the Near East, with shading representing the difference between the parameter settings of anatomically modern humans (AMH) and Eurasian Archaic humans (EAH); a total of 15,200 agent-based model simulations were run with a wide variety of AMH–EAH settings, each forced with NPP data in panel **a**. **c**, As in panel **b**, but for the Arabian Peninsula. **d**, As in panel **b**, but for the Balkans. **e**, As in panel **b**, but for Central Europe. **f**, As in panel **b**, but for Denisova cave. **g**, As in panel **b**, but for Southeast Asia. Arrows with labels indicate the earliest direct archaeological evidence for presence of *H. sapiens*. Agent-based model simulations driven with climate data simulate realistic arrival times across Eurasia for a range of different parameters. LGM, Last Glacial Maximum. Figure adapted with permission from ref. 20.

during a period of colder and more seasonal environmental conditions[142]. The succession of archaeological technocomplexes in France between 32 and 21 ka has also been linked to climate shifts[143].

Evidence linking the cultural innovation of fire use to climate change is more limited. The earliest evidence for the use of fire dates back more than a million years to sites at Lake Baringo (Kenya) and Gadeb (Ethiopia[144,145]). Traces of systematic burning and cooking of fish were found at Gesher Benot Ya'aqov in the Levant, dated to about 800 ka (ref. 146). The intentional use of fire became much more frequent and geographically widespread (albeit with considerable gaps

in the record) from about 400 ka (ref. 147). Although the impact of fire on human evolution is usually associated with the importance of cooking food[148], fire use for heat production probably aided the dispersal from tropical areas into colder subtropical and extratropical regions[149–151].

Clothing is as important as heat production to live in cold habitats but has a negligible chance of being fossilized[152]. However, the manufacture of clothing requires the production of tools such as hide scrapers and awls, which have survived in the archaeological record. Hide scrapers might be at least as old as 780 ka (ref. 153), whereas awls — made to pierce soft materials such as hide for clothing and the production of carrying bags — probably date from as early as the Middle Stone Age[154,155]. Evidence for clothing, sandals and basketry dates back to the Last Glacial Maximum, 21 ka (ref. 156). Given that these tools (except the hide scrapers, which are made from lithic flakes) are crafted from raw material with little potential for preservation, it is conceivable that their earliest appearance in the archaeological record is well after the actual emergence of their production.

Shelters made of wood or other biological materials also probably enabled colonization of colder climates. Early human-made structures date back at least to 476 ka (ref. 157), yet, although probably common, are extremely rare in the archaeological record. Thus, it seems plausible that the use of fire (for heating), the construction of shelters, and the production of fitted clothing (for insulation) could have been invented much earlier than the Middle Stone Age, as further suggested by the very early colonization of Northern Europe around 700 ka (ref. 125). Although there is evidence for temperate conditions there at that time[125], palaeoclimate modelling indicates winter temperatures close to −10 °C, which is well below human physiological tolerance limits without clothing or fur bedding[158] (Fig. 7a).

The dating uncertainties in archaeological sequences, the paucity of samples and the often-ambiguous interpretations of palaeoclimate reconstructions make it challenging to determine whether climate changes caused regional or large-scale cultural shifts. Species distribution models can be used to further elucidate how hominins adapted to cold climates by exploring the linkage of cultural innovation to climate niche expansion. The problem can be recast in terms of examining the evolution of the human climate niche under a phylogenetically explicit context[56,159]. *Homo heidelbergensis*, *H. neanderthalensis* and *H. sapiens* form a distinct clade of species whose climate niches greatly exceeded the limits of earlier hominins[3,21] (Fig. 7a). This interpretation is consistent with the expansion of their biome preferences (Fig. 5d–f). Because the niche limits explored by these species exceeded the physiological tolerance limits of earlier humans, it is conceivable they might have used fire for heating, built cold-proof shelters and used fitted clothes to protect themselves under low environmental temperatures. The notion that at least *H. neanderthalensis* and *H. sapiens* culturally adapted to climate stress by developing behavioural plasticity is further supported by their peculiar foraging strategies, which were extraordinarily flexible in their resource use.

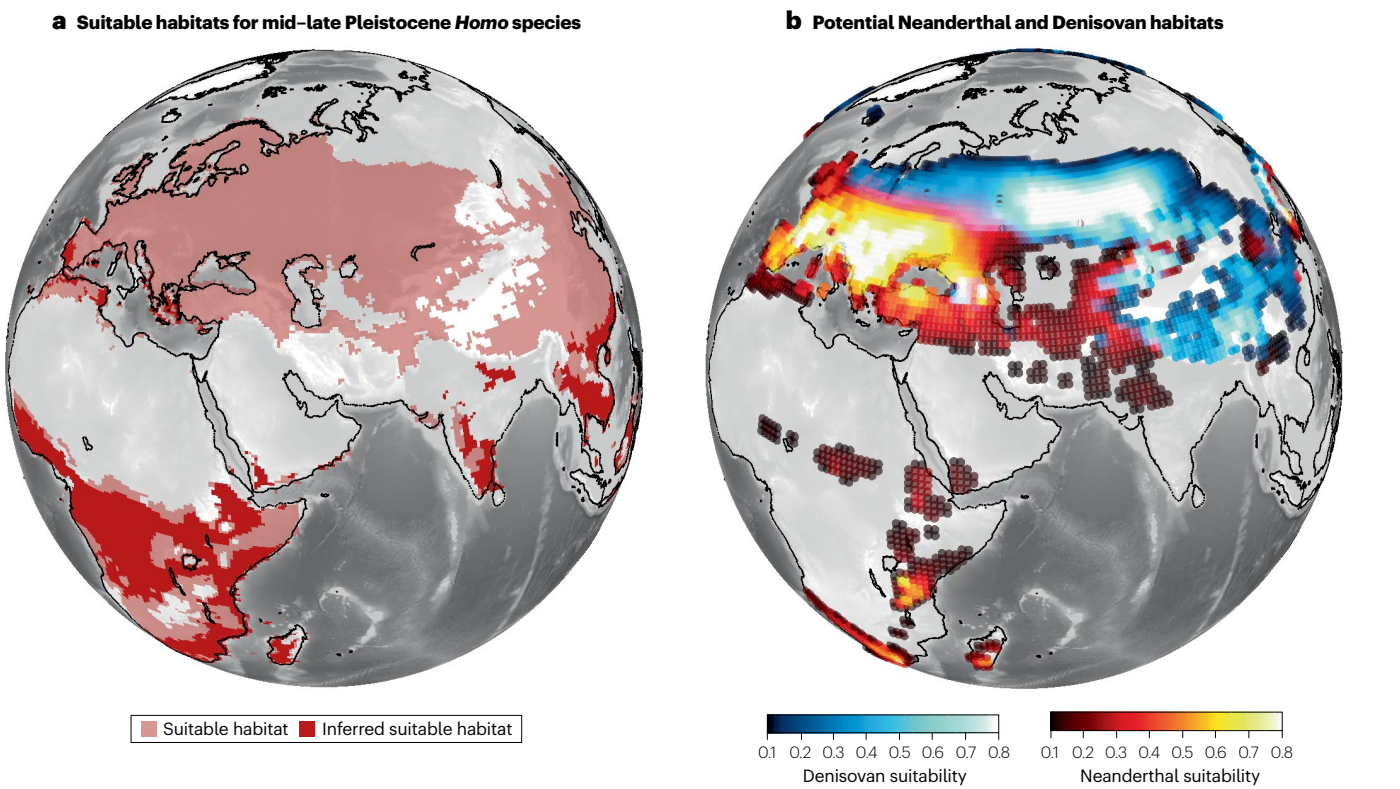

Fig. 7 | Habitat preferences. a, The geographical distribution of suitable habitats (light red shading) and inferred suitable habitats (dark red shading) for middle to late Pleistocene *Homo* species (*H. heidelbergensis*, *H. neanderthalensis* and *H. sapiens*); inferred habitats are derived assuming a constant rate of climate niche evolution across the *Homo* family tree. **b**, Potential Neanderthal and Denisovan habitats[22], with overlapping regions highlighting possible time-average interbreeding areas. Habitat analysis of different human species can provide crucial information on their origins, phylogenetic relations, encounters and interactions.

Both species exploited a far wider resources spectrum than earlier *Homo* species and invented weapons to aid in hunting large game animals[106,160,161].

Summary and future perspectives

This Review has synthesized quantitative efforts to understand how past climate shifts shaped the evolutionary trajectory of the human genus. Rainfall and net primary productivity shifts generated by the axis wobble (precession) of Earth (Fig. 2) affected the African/Eurasian dispersal of human species and probably also the subsequent history of multispecies interactions (Fig. 6), including extinctions and likely interbreeding events (Fig. 7b). The expansion and diversification of the hominin climate niche towards colder climates (Fig. 7a) is an important proxy for climate-related adaptations in multiple *Homo* species. This diversification was further aided by cultural adaptation events during the middle to late Pleistocene including the controlled use of fire, the use of clothing and the development of more sophisticated tools to hunt extratropical megafauna and increase the protein intake[15]. Further climate variability (Fig. 1) opened otherwise submerged land bridges, allowing important dispersals[162] into Indonesia (across the Sunda shelf), Australia (across the Sahul shelf) and the Americas (across the Bering Strait).

This Review also introduced several modelling techniques that can be used to examine different aspects of evolution (Fig. 4a). Combining habitat models that capture the transient history of our environment with estimates of net primary productivity or population growth rate can obtain more realistic and empirically informed estimates of carrying capacity for different species or their demographic characteristics. This information is crucial as input to density-based F–KPP and agent-based models and can be used in the future to examine multispecies interactions, such as competition, cultural transfer or interbreeding. The field of quantitative climatological anthropology is still in its infancy, and the modelling-based insight has great potential. Several promising avenues to advance knowledge of climate impacts on human evolution are now discussed.

Simulating competition and culture

Previously, density-based F–KPP models were introduced only in their simplest form. These models can be further expanded by introducing additional terms to simulate the dynamics of multispecies populations[25,163], predator–prey interactions[164] and even the emergence of culture[165]. To capture the interaction between different species, either through competition[163,166–169] or interbreeding[25], the basic single-species model can be extended to a multispecies system[170,171]:

$$\frac{\partial \rho_i}{\partial t} = \nabla(\kappa_i \nabla \rho_i) + \alpha_i \rho_i \left(1 - \frac{\rho_i + \sum_{i \neq j} \beta_j \rho_j}{K_i}\right) + \sum_{i \neq j} F_{ij}(\rho_i, \rho_j), \qquad (2)$$

in which β_j represents the competitive advantage of species j over species i. F_{ij} captures further interaction dynamics, such as interbreeding, predation or spreading of diseases and related mortality.

To further enhance the realism of this approach, a species-specific property c_i can be introduced that increases carrying capacity[165] $K_i \rightarrow K_i(1 + c_i)$ and accounts for processes that improve survival relative to other groups. These processes include hunting success, social skills, innovation and tool sophistication, and c_i can therefore be interpreted broadly as a metric of culture and $K_i(1 + c_i)$ as cultural carrying capacity. Mathematically, the temporal change of culture $\dot{c}_i$ is due to random innovations or knowledge recombinations $\zeta(t)$ with a given distribution, whereas the loss of culture can be parameterized by a resistance term $-\lambda_i c_i$, which characterizes the imperfect cultural transfer from one generation to another. Smaller values of λ_i (larger damping timescales) are associated with a stronger intergenerational knowledge transfer, which might occur in groups with higher cognitive, language and social learning abilities. The simplified zero-dimensional ordinary differential equation for the evolution of culture[172] can then be expressed through an Ornstein–Uhlenbeck process, describing Brownian motion[173,174] as $\dot{c}_i = -\lambda_i c_i + \zeta(t)$. In a more realistic 2D context, the time evolution of culture can be further described by a reaction–diffusion equation, with a spatial diffusivity κ_i^c and a state-dependent (multiplicative) stochastic innovation term $\zeta(t)I(\rho_i, c_i)$ that depends on the population densities ρ_i, as suggested in the cumulative cultural evolution model[175,176], or on the pre-existing culture c_i. The cumulative evolution of culture might be further accelerated when habitat tracking is not an available option and when environmental stress σ_i induces adaptation pressure. In addition to a state dependence of $\lambda_i(c_i)$, one can further introduce a cultural interaction term $G_{ij}(c_i, c_j)$ between different populations, which accounts for the fact that hominin groups can learn from each other and adopt the cultural advances made by another group — a process that is not captured by the diffusion of knowledge and culture within one group. The final dynamical time-evolving culture reaction–diffusion equation, which also parameterizes adaptation pressure σ_i, can then be written as:

$$\frac{\partial c_i}{\partial t} = \nabla(\kappa_i^c \nabla c_i) - \lambda_i(c_i)c_i + I(\rho_i, c_i)\zeta(t)[\sigma_i + \varepsilon] + \sum_{i \neq j} G_{ij}(c_i, c_j) \qquad (3)$$

The coupled multispecies–culture reaction–diffusion equations (equations (1)–(3)) are introduced here in a symbolic way to illustrate the fact that specific human traits, habitat preferences and interactions (equations (2) and (3)), as well as adaptation to environmental stress, can in principle be modelled mathematically. They can be run for different climate conditions represented by $K_i(x, y, t)$, $\sigma_i(x, y, t)$ and demographic and cultural parameters $(\alpha_i, \kappa_i, \beta_i, \kappa_i^c, \lambda_i)$ to obtain the time evolution of species densities ρ_i, culture c_i as well as their coupling in terms of $I(\rho_i, c_i)$ and $K_i(c_i)$. Equations (1–3) provide a more versatile framework to simulate spatiotemporal aspects[165,177] of human cultural evolution than previous non-spatial models[176], which do not include the explicit dynamical coupling between climate, culture, and population density. Future research using such mathematical approaches will help to quantify the drivers of hominin adaptation, survival and competition and might provide clues to the emergence of culture and transitions, as well as the late near-exponential cumulative growth in culture since the Anthropocene. One of the key challenges will be to extract realistic parameters for extended multispecies reaction–diffusion models from empirical evidence, but the overall approach holds great potential.

Climate effects on human genomics

Phylogenetically close species often share genes with each other. The introgressed genes can be detrimental to survival, but on occasion they can be fixed in the receiving population if they confer some fitness advantage. Modern-day humans carry in their genome a small quantity of DNA deriving from other human species[178]. Although most introgressed alleles must have been lost over time via drift and/or purifying selection[179], in some human populations specific introgressed alleles are conserved at comparatively high frequencies. For example, alleles conferring high altitude resistance are positively selected for

in Tibetans[180,181], and alleles conferring resistance to tropical diseases are positively selected for in Papuans[182].

Combining the modelling approaches described previously with palaeogenomic data will advance the current understanding of the climate change impacts on human evolution, speciation and genetic diversification and further elucidate the origins of the genetic makeup of present-day humans[183]. For instance, because Denisovans were first identified in South Siberia and lived there during full glacial conditions some 50 ka (ref. 184), they were long considered a cold-climate-adapted variant of the human lineage, a trait once attributed to Neanderthals. Yet the high frequency of Denisovan alleles in modern-day humans from Papua and the Philippines[185,186] challenges the cold-adaptation hypothesis. Denisovans were much more adapted to cold environments, characterized by boreal forests and even tundra, whereas their Neanderthal cousins preferred warmer temperate forests and grassland[22] (Fig. 5). The two species were normally separated geographically, with Neanderthals typically preferring southwestern Eurasia and Denisovans the northeast. However, during warm interglacial periods (Fig. 2), the habitats of these two groups began to overlap geographically (Fig. 7b), which would have increased the chances of interbreeding. The calculation of past habitat overlaps identified four potential interbreeding episodes at ~78, 120, 210 and 320 ka. The first two warm-period interbreeding windows agree well with palaeogenetic data, thereby supporting the notion that climate-driven and CO_2-driven shifts in vegetation patterns (Fig. 3b,c) brought together different human populations, with long-term repercussions on human genetic diversification. Future quantitative modelling approaches that address pre-conditioning factors for interbreeding or that simulate genetics specifically[23,183,187] can help resolve open questions regarding genetic admixtures between hominins.

Improved quantification of climate-human interactions

To better estimate the uncertainties inherent to these model-based inferences, due to limited knowledge in climate conditions, phylogenetic dependencies or human responses, future research should use multimodel ensemble techniques[188], Bayesian methods[6] or multiparameter simulations[20,71] (Fig. 6).

An interesting question that remains to be addressed is whether the modelling frameworks described above can be further modified to describe the more complex bidirectional human–environmental interactions that characterize the Anthropocene[189]. Since the advent of farming and industrialization, humans have started to extract more resources from the environment. Instead of using a prescribed carrying capacity K in equation (1) (or variants thereof), a better approach would be to formulate a dynamical equation for K, that includes a density-dependent resource depletion term[172,190], and a resource sharing parameterization that describes the effect of global trade among different regions.

Addressing the issue of future climate-mediated human responses with quantitative methods that were tested on past conditions might open new possibilities to explore adaptation and conservation pathways in the face of anthropogenic climate change, resource depletion, food insecurity and transgression of planetary boundaries[191].

Published online: 12 September 2024

References

1. Margari, V. et al. Extreme glacial cooling likely led to hominin depopulation of Europe in the early Pleistocene. *Science* **381**, 693–699 (2023).
2. Maslin, M. A., Shultz, S. & Trauth, M. H. A synthesis of the theories and concepts of early human evolution. *Phil. Trans. R. Soc. B* **370**, 20140064 (2015).
3. Zeller, E., Timmermann, A., Yun, K., Raia, P. & Ruan, J. Human adaptation to diverse biomes over the past 3 million years. *Science* **380**, 604–608 (2023).
4. Beyer, R. M., Krapp, M., Eriksson, A. & Manica, A. Climatic windows for human migration out of Africa in the past 300,000 years. *Nat. Commun.* **12**, 4889 (2021).
5. Timmermann, A. & Friedrich, T. Late Pleistocene climate drivers of early human migration. *Nature* **538**, 92–95 (2016).
6. Degroot, D. et al. The history of climate and society: a review of the influence of climate change on the human past. *Environ. Res. Lett.* **17**, 103001 (2022).
7. Ludecke, T. et al. Persistent C-3 vegetation accompanied Plio-Pleistocene hominin evolution in the Malawi Rift (Chiwondo Beds, Malawi). *J. Hum. Evol.* **90**, 163–175 (2016).
8. Cerling, T. E. et al. Woody cover and hominin environments in the past 6 million years. *Nature* **476**, 51–56 (2011).
9. Cerling, T. E., Quade, J., Wang, Y. & Bowman, J. R. Carbon isotopes in soils and palaeosols as ecology and palaeoecology indicators. *Nature* **341**, 138–139 (1989).
10. Lee-Thorp, J. A., Sponheimer, M., Passey, B. H., de Ruiter, D. J. & Cerling, T. E. Stable isotopes in fossil hominin tooth enamel suggest a fundamental dietary shift in the Pliocene. *Phil. Trans. R. Soc. B* **365**, 3389–3396 (2010).
11. Feakins, S. J. et al. Northeast African vegetation change over 12 m.y. *Geology* **41**, 295–298 (2013).
12. Tierney, J. E., deMenocal, P. B. & Zander, P. D. A climatic context for the out-of-Africa migration. *Geology* **45**, 1023–1026 (2017).
13. DeMenocal, P. B. Plio-Pleistocene African climate. *Science* **270**, 53–59 (1995).
14. Scott, L. & Neumann, F. H. Pollen-interpreted palaeoenvironments associated with the Middle and Late Pleistocene peopling of southern Africa. *Quat. Int.* **495**, 169–184 (2018).
15. Jaouen, K. et al. Exceptionally high $\delta^{15}N$ values in collagen single amino acids confirm Neandertals as high-trophic level carnivores. *Proc. Natl Acad. Sci. USA* **116**, 4928–4933 (2019).
16. Behrensmeyer, A. K. Climate change and human evolution. *Science* **311**, 476–478 (2006).
17. Smith, R. & Gregory, J. The last glacial cycle: transient simulations with an AOGCM. *Clim. Dynam.* **38**, 1545–1559 (2012).
18. Yun, K.-S. et al. A transient CGCM simulation of the past 3 million years. *Clim. Past.* **19**, 1951–1974 (2023).
19. Timmermann, A. et al. Modeling obliquity and CO_2 effects on Southern Hemisphere climate during the past 408 ka. *J. Clim.* **27**, 1863–1875 (2014).
20. Vahdati, A. R., Weissmann, J. D., Timmermann, A., de Leon, M. P. & Zollikofer, C. P. E. Exploring Late Pleistocene hominin dispersals, coexistence and extinction with agent-based multi-factor models. *Quat. Sci. Rev.* **279**, 107391 (2022).
21. Timmermann, A. et al. Climate effects on archaic human habitats and species successions. *Nature* **604**, 495–501 (2022).
22. Ruan, J. et al. Climate shifts orchestrated hominin interbreeding events across Eurasia. *Science* **381**, 699–703 (2023).
23. Eriksson, A. et al. Late Pleistocene climate change and the global expansion of anatomically modern humans. *Proc. Natl Acad. Sci. USA* **109**, 16089–16094 (2012).
24. Raia, P. et al. Past extinctions of Homo Species coincided with increased vulnerability to climatic change. *One Earth* **3**, 480–490 (2020).
25. Timmermann, A. Quantifying the potential causes of Neanderthal extinction: abrupt climate change versus competition and interbreeding. *Quat. Sci. Rev.* **238**, 106331 (2020).
26. Willeit, M., Ganopolski, A., Calov, R. & Brovkin, V. Mid-Pleistocene transition in glacial cycles explained by declining CO_2 and regolith removal. *Sci. Adv.* **5**, eaav7337 (2019).
27. Liu, Z. et al. Transient simulation of last deglaciation with a new mechanism for Bølling–Allerød warming. *Science* **325**, 310–314 (2009).
28. Menviel, L., Timmermann, A., Timm, O. & Mouchet, E. A. Deconstructing the last glacial termination: the role of millennial and orbital-scale forcings. *Quat. Sci. Rev.* **30**, 1155–1172 (2011).
29. Menviel, L., Timmermann, A., Friedrich, T. & England, M. H. Hindcasting the continuum of Dansgaard–Oeschger variability: mechanisms, patterns and timing. *Clim. Past.* **10**, 63–77 (2014).
30. Friedrich, T., Timmermann, A., Tigchelaar, M., Timm, O. E. & Ganopolski, A. Nonlinear climate sensitivity and its implications for future greenhouse warming. *Sci. Adv.* **2**, e1501923 (2016).
31. Singarayer, J. S. & Valdes, P. J. High-latitude climate sensitivity to ice-sheet forcing over the last 120 kyr. *Quat. Sci. Rev.* **29**, 43–55 (2010).
32. Kapsch, M. L., Mikolajewicz, U., Ziemen, F. & Schannwell, C. Ocean response in transient simulations of the last deglaciation dominated by underlying ice-sheet reconstruction and method of meltwater distribution. *Geophys. Res. Lett.* **49**, e2021GL096767 (2022).
33. Ganopolski, A., Brovkin, V. & Calov, R. Simulation of glacial–interglacial atmospheric CO_2 variations using a comprehensive Earth system model of intermediate complexity. *Goechim. Cosmochim. Acta* **73**, A411–A411 (2009).
34. Krapp, M., Beyer, R. M., Edmundson, S. L., Valdes, P. J. A. & Manica, A. A statistics-based reconstruction of high-resolution global terrestrial climate for the last 800,000 years. *Sci. Data* **8**, 228 (2021).
35. Leonardi, M., Hallett, E. Y., Beyer, R., Krapp, M. & Manica, A. pastclim 1.2: an R package to easily access and use paleoclimatic reconstructions. *Ecography* **2023**, e06481 (2023).
36. Barreto, E., Holden, P. B., Edwards, N. R. & Rangel, T. F. PALEO-PGEM-Series: a spatial time series of the global climate over the last 5 million years (Plio-Pleistocene). *Glob. Ecol. Biogeog.* **32**, 1034–1045 (2023).
37. Gibert, C. et al. Climate-inferred distribution estimates of mid-to-late Pliocene hominins. *Glob. Planet. Change* **210**, 103756 (2022).

38. Burke, A. et al. Risky business: the impact of climate and climate variability on human population dynamics in Western Europe during the Last Glacial Maximum. *Quat. Sci. Rev.* **164**, 217–229 (2017).
39. Klein, K. et al. Human existence potential in Europe during the Last Glacial Maximum. *Quat. Int.* **581–582**, 7–27 (2021).
40. Banks, W. E. et al. An ecological niche shift for Neanderthal populations in Western Europe 70,000 years ago. *Sci. Rep.* **11**, 5346 (2021).
41. Barve, N. et al. The crucial role of the accessible area in ecological niche modeling and species distribution modeling. *Ecol. Model.* **222**, 1810–1819 (2011).
42. Elith, J. et al. A statistical explanation of MaxEnt for ecologists. *Div. Distrib.* **17**, 43–57 (2011).
43. Breiman, L. Random forests. *Mach. Learn.* **45**, 5–32 (2001).
44. Hirzel, A. H., Hausser, J., Chessel, D. & Perrin, N. Ecological-niche factor analysis: how to compute habitat-suitability maps without absence data? *Ecology* **83**, 2027–2036 (2002).
45. Prentice, I. C. et al. A global biome model based on plant physiology and dominance, soil properties and climate. *J. Biogeogr.* **19**, 117–134 (1992).
46. Carotenuto, F. et al. MInOSSE: a new method to reconstruct geographic ranges of fossil species. *Methods Ecol. Evol.* **11**, 1121–1132 (2020).
47. Mondanaro, A. et al. ENphylo: a new method to model the distribution of extremely rare species. *Methods Ecol. Evol.* **14**, 911–922 (2023).
48. Tikhonov, G. et al. Joint species distribution modelling with the r-package Hmsc. *Methods Ecol. Evol.* **11**, 442–447 (2020).
49. Midgley, G. F. & Thuiller, W. Global environmental change and the uncertain fate of biodiversity. *N. Phytol.* **167**, 638–641 (2005).
50. Hengl, T., Sierdsema, H., Radovic, A. & Dilo, A. Spatial prediction of species' distributions from occurrence-only records: combining point pattern analysis, ENFA and regression-kriging. *Ecol. Model.* **220**, 3499–3511 (2009).
51. Santini, L., Benitez-Lopez, A., Maiorano, L., Cengic, M. & Huijbregts, M. A. J. Assessing the reliability of species distribution projections in climate change research. *Divers. Distrib.* **27**, 1035–1050 (2021).
52. Jimenez-Valverde, A. Sample size for the evaluation of presence–absence models. *Ecol. Indic.* **114**, 106289 (2020).
53. Qiao, H. et al. An evaluation of transferability of ecological niche models. *Ecography* **42**, 521–534 (2019).
54. Soberón, J. & Nakamura, M. Niches and distributional areas: concepts, methods, and assumptions. *Proc. Natl Acad. Sci. USA* **106**, 19644–19650 (2009).
55. Mondanaro, A. et al. The role of habitat fragmentation in Pleistocene megafauna extinction in Eurasia. *Ecography* **44**, 1619–1630 (2021).
56. Mondanaro, A. et al. A major change in rate of climate niche envelope evolution during hominid history. *iScience* **23**, 101693 (2020).
57. Steele, J. Human dispersals: mathematical models and the archaeological record. *Hum. Biol.* **81**, 121–140 (2009).
58. Liu, P. P. An analysis of a predator-prey model with both diffusion and migration. *Math. Comput. Model.* **51**, 1064–1070 (2010).
59. Vlad, M. O., Cavalli-Sforza, L. L. & Ross, J. Enhanced (hydrodynamic) transport induced by population growth in reaction-diffusion systems with application to population genetics. *Proc. Natl Acad. Sci. USA* **101**, 10249–10253 (2004).
60. Verhulst, P. F. Notice sur la loi que la population suit dans son accroissement. *Corresp. Math. Phys.* **10**, 113–121 (1838).
61. Fort, J., Pujol, T. & Cavalli-Sforza, L. L. Palaeolithic populations and waves of advance (human range expansions). *Camb. Archaeol. J.* **14**, 53–61 (2004).
62. Young, D. A. & Bettinger, R. L. Simulating the global human expansion in the Late Pleistocene. *J. Archaeol. Sci.* **22**, 89–92 (1995).
63. Steele, J., Adams, J. & Sluckin, T. Modelling Paleoindian dispersals (paleoecology and human populations). *World Archaeol.* **30**, 286–305 (1998).
64. Pinhasi, R., Fort, J. & Ammerman, A. J. Tracing the origin and spread of agriculture in Europe. *PLoS Biol.* **3**, 2220–2228 (2005).
65. Ammerman, A. J. & Cavalli-Sforza, L. L. Measuring the rate of spread of early farming in Europe. *Man* **6**, 674–688 (1971).
66. Szabo, C. & Teo, Y. M. Formalization of weak emergence in multiagent systems. *ACM Trans. Model. Comp. Simul.* **26**, 1–25 (2015).
67. Bedau, M. A. Weak emergence. *Noûs* **31**, 375–399 (1997).
68. Axtell, R. L. et al. Population growth and collapse in a multiagent model of the Kayenta Anasazi in Long House Valley. *Proc. Natl Acad. Sci. USA* **99**, 7275–7279 (2002).
69. Janssen, M. A. & Ostrom, E. Empirically based, agent-based models. *Ecol. Soc.* **11**, 37 (2006).
70. Helbing, D. & Yu, W. J. The outbreak of cooperation among success-driven individuals under noisy conditions. *Proc. Natl Acad. Sci. USA* **106**, 3680–3685 (2009).
71. Vahdati, A. R., Weissmann, J. D., Timmermann, A., de Leon, M. S. P. & Zollikofer, C. P. E. Drivers of Late Pleistocene human survival and dispersal: an agent-based modeling and machine learning approach. *Quat. Sci. Rev.* **221**, 105867 (2019).
72. Barton, C. M. & Riel-Salvatore, J. Agents of change: modeling biocultural evolution in Upper Pleistocene western Eurasia. *Adv. Comp. Syst* **15**, 1150003 (2012).
73. Wren, C. D. & Burke, A. Habitat suitability and the genetic structure of human populations during the Last Glacial Maximum (LGM) in Western Europe. *PLoS ONE* **14**, e0217996 (2019).
74. Berger, A. Long-term variations of caloric insolation resulting from the Earth's orbital elements. *Quat. Res.* **9**, 139–167 (1978).
75. Cheng, H. et al. Milankovitch theory and monsoon. *Innovation* **3**, 100338 (2022).
76. Tigchelaar, M. & Timmermann, A. Mechanisms rectifying the annual mean response of tropical Atlantic rainfall to precessional forcing. *Clim. Dyn.* **47**, 271–293 (2016).
77. Braconnot, P., Marzin, C., Grégoire, L., Mosquet, E. & Marti, O. Monsoon response to changes in Earth's orbital parameters: comparisons between simulations of the Eemian and of the Holocene. *Clim. Past.* **4**, 281–294 (2008).
78. Cheng, H. et al. The Asian monsoon over the past 640,000 years and ice age terminations. *Nature* **534**, 640–646 (2016).
79. Claussen, M., Fohlmeister, J., Ganopolski, A. & Brovkin, V. Vegetation dynamics amplifies precessional forcing. *Geophy. Res. Lett.* **33**, L09709 (2006).
80. Scholz, C. A. et al. East African megadroughts between 135 and 75 thousand years ago and bearing on early-modern human origins. *Proc. Natl Acad. Sci. USA* **104**, 16416–16421 (2007).
81. Tachikawa, K. et al. The precession phase of hydrological variability in the Western Pacific Warm Pool during the past 400 ka. *Quat. Sci. Rev.* **30**, 3716–3727 (2011).
82. Schneider, T., Bischoff, T. & Haug, G. H. Migrations and dynamics of the intertropical convergence zone. *Nature* **513**, 45–53 (2014).
83. Ai, H. et al. Concurrent Asian monsoon strengthening and early modern human dispersal to East Asia during the last interglacial. *Proc. Natl Acad. Sci. USA* **121**, e2308994121 (2024).
84. Armitage, S. J. et al. The southern route 'Out of Africa': evidence for an early expansion of modern humans into Arabia. *Science* **331**, 453–456 (2011).
85. Castaneda, I. S. et al. Wet phases in the Sahara/Sahel region and human migration patterns in North Africa. *Proc. Natl Acad. Sci. USA* **106**, 20159–20163 (2009).
86. Clark, P. U. et al. The middle Pleistocene transition: characteristics, mechanisms, and implications for long-term changes in atmospheric pCO_2. *Quat. Sci. Rev.* **25**, 3150–3184 (2006).
87. Dansgaard, W. et al. Evidence for general instability of past climate from a 250-kyr ice-core record. *Nature* **364**, 218–220 (1993).
88. Deplazes, G. et al. Links between tropical rainfall and North Atlantic climate during the last glacial period. *Nat. Geosci.* **6**, 213–217 (2013).
89. Litt, T., Pickarski, N., Heumann, G., Stockhecke, M. & Tzedakis, P. A 600,000 year long continental pollen record from Lake Van, eastern Anatolia (Turkey). *Quat. Sci. Rev.* **104**, 30–41 (2014).
90. Stockhecke, M. et al. Millennial to orbital-scale variations of drought intensity in the Eastern Mediterranean. *Quat. Sci. Rev.* **150**, 312–314 (2016).
91. Schulz, M., Berger, W. H., Sarnthein, M. & Grootes, P. M. Amplitude variations of 1470-year climate oscillations during the last 100,000 years linked to fluctuations of continental ice mass. *Geophy. Res. Lett.* **26**, 3385–3388 (1999).
92. Menviel, L. C., Skinner, L. C., Tarasov, L. & Tzedakis, P. C. An ice-climate oscillatory framework for Dansgaard–Oeschger cycles. *Nat Rev. Earth. Environ.* **1**, 677–693 (2020).
93. Stocker, T. & Johnsen, S. A minimum thermodynamic model for the bipolar seesaw. *Paleoceanography* **18**, 1087 (2003).
94. Timmermann, A., Gildor, H., Schulz, M. & Tziperman, E. Coherent resonant millennial-scale climate oscillations triggered by massive meltwater pulses. *J. Clim.* **16**, 2569–2585 (2003).
95. Ganopolski, A. & Rahmstorf, S. Rapid changes of glacial climate simulated in a coupled climate model. *Nature* **409**, 153–158 (2001).
96. Armstrong, E., Izumi, K. & Valdes, P. Identifying the mechanisms of DO-scale oscillations in a GCM: a salt oscillator triggered by the Laurentide ice sheet. *Clim. Dyn.* **60**, 3983–4001 (2022).
97. Izumi, K., Armstrong, E. & Valdes, P. Global footprints of Dansgaard–Oeschger oscillations in a GCM. *Quat. Sci. Rev.* **305**, 108016 (2023).
98. Kuniyoshi, Y., Abe-Ouchi, A., Sherriff-Tadano, S., Chan, W. L. & Saito, F. Effect of climatic precession on Dansgaard–Oeschger-like oscillations. *Geophys. Res. Lett.* **49**, e2021GL095695 (2022).
99. Vettoretti, G. & Peltier, W. R. Fast physics and slow physics in the nonlinear Dansgaard–Oeschger relaxation oscillation. *J. Clim.* **31**, 3423–3449 (2018).
100. Schulz, M., Paul, A. & Timmermann, A. Relaxation oscillators in concert: a framework for climate change at millennial timescales during the late Pleistocene. *Geophys. Res. Lett.* **29**, 46-1–46-4 (2002).
101. Abshagen, J. & Timmermann, A. An organizing center for thermohaline excitability. *J. Phys. Ocean.* **34**, 2756–2760 (2004).
102. van Kreveld, S. et al. Potential links between surging ice sheets, circulation changes, and the Dansgaard–Oeschger cycles in the Irminger Sea, 60–18 Kyr. *Paleoceanography* **15**, 425–442 (2000).
103. Bond, G. et al. Correlations between climate records from North Atlantic sediments and Greenland ice. *Nature* **365**, 143–147 (1993).
104. Harrison, S. P. & Prentice, A. I. Climate and CO_2 controls on global vegetation distribution at the last glacial maximum: analysis based on palaeovegetation data, biome modelling and palaeoclimate simulations. *Glob. Change Biol.* **9**, 983–1004 (2003).
105. Jennings, R. P. et al. The greening of Arabia: multiple opportunities for human occupation of the Arabian Peninsula during the Late Pleistocene inferred from an ensemble of climate model simulations. *Quat. Int.* **382**, 181–199 (2015).
106. Potts, R. et al. Increased ecological resource variability during a critical transition in hominin evolution. *Sci. Adv.* **6**, eabc8975 (2020).
107. Melchionna, M. et al. Fragmentation of Neanderthals' pre-extinction distribution by climate change. *Palaeog. Palaeoclim. Palaeoecol.* **496**, 146–154 (2018).
108. Miller, J. M. & Wang, Y. M. V. Ostrich eggshell beads reveal 50,000-year-old social network in Africa. *Nature* **601**, 234–239 (2022).

109. Graham, C. H., VanDerWal, J., Phillips, S. J., Moritz, C. & Williams, S. E. Dynamic refugia and species persistence: tracking spatial shifts in habitat through time. *Ecography* **33**, 1062–1069 (2010).
110. Eldredge, N. et al. The dynamics of evolutionary stasis. *Paleobiology* **31**, 133–145 (2005).
111. Raia, P., Passaro, F., Fulgione, D. & Carotenuto, F. Habitat tracking, stasis and survival in Neogene large mammals. *Biol. Lett.* **8**, 64–66 (2012).
112. Dart, R. A. *Australopithecus africanus*: the man-ape of South Africa. *Nature* **115**, 195–199 (1925).
113. Dominguez-Rodrigo, M. Is the 'Savanna Hypothesis' a dead concept for explaining the emergence of the earliest hominins? *Curr. Anthropol.* **55**, 59–81 (2014).
114. Reed, K. E. Early hominid evolution and ecological change through the African Plio-Pleistocene. *J. Hum. Evol.* **32**, 289–322 (1997).
115. White, T. D. et al. *Ardipithecus ramidus* and the paleobiology of early hominids. *Science* **326**, 75–86 (2009).
116. Haywood, A. M. & Valdes, P. J. Vegetation cover in a warmer world simulated using a dynamic global vegetation model for the Mid-Pliocene. *Palaeogeogr. Palaeoclimatol. Palaeoecol.* **237**, 412–427 (2006).
117. Grove, M. Speciation, diversity, and Mode 1 technologies: the impact of variability selection. *J. Hum. Evol.* **61**, 306–319 (2011).
118. Potts, R. & Faith, J. T. Alternating high and low climate variability: the context of natural selection and speciation in Plio-Pleistocene hominin evolution. *J. Hum. Evol.* **87**, 5–20 (2015).
119. Grove, M. et al. Climatic variability, plasticity, and dispersal: a case study from Lake Tana, Ethiopia. *J. Hum. Evol.* **87**, 32–47 (2015).
120. Grove, M. Evolution and dispersal under climatic instability: a simple evolutionary algorithm. *Adapt. Behav.* **22**, 235–254 (2014).
121. Martin, J. M., Leece, A. B., Baker, S. E., Herries, A. I. R. & Strait, D. S. A lineage perspective on hominin taxonomy and evolution. *Evol. Anthropol.* **33**, e22018 (2024).
122. Gabunia, L. et al. Earliest Pleistocene hominid cranial remains from Dmanisi, Republic of Georgia: taxonomy, geological setting, and age. *Science* **288**, 1019–1025 (2000).
123. Scardia, G. et al. Chronologic constraints on hominin dispersal outside Africa since 2.48 Ma from the Zarqa Valley, Jordan. *Quat. Sci. Rev.* **219**, 1–19 (2019).
124. Hilgen, S. L. et al. Revised age and stratigraphy of the classic *Homo erectus*-bearing succession at Trinil (Java, Indonesia). *Quat. Sci. Rev.* **301**, 107908 (2023).
125. Parfitt, S. A. et al. Early Pleistocene human occupation at the edge of the boreal zone in northwest Europe. *Nature* **466**, 229–233 (2010).
126. Liu, W. et al. The earliest unequivocally modern humans in southern China. *Nature* **526**, 696–699 (2015).
127. Brumm, A. et al. Oldest cave art found in Sulawesi. *Sci. Adv.* **7**, eabd4648 (2021).
128. Harvati, K. et al. Apidima Cave fossils provide earliest evidence of *Homo sapiens* in Eurasia. *Nature* **571**, 500–504 (2019).
129. Hershkovitz, I. et al. The earliest modern humans outside Africa. *Science* **359**, 456–459 (2018).
130. Pigati, J. S. et al. Independent age estimates resolve the controversy of ancient human footprints at White Sands. *Science* **382**, 73–75 (2023).
131. Leroy, S. A. G., Arpe, K. & Mikolajewicz, U. Vegetation context and climatic limits of the Early Pleistocene hominin dispersal in Europe. *Quat. Sci. Rev.* **30**, 1448–1463 (2011).
132. Anton, S. C., Leonard, W. R. & Robertson, M. L. An ecomorphological model of the initial hominid dispersal from Africa. *J. Hum. Evol.* **43**, 773–785 (2002).
133. Staubwasser, M. et al. Impact of climate change on the transition of Neanderthals to modern humans in Europe. *Proc. Natl Acad. Sci. USA* **115**, 9116–9121 (2018).
134. Greenbaum, G. et al. Disease transmission and introgression can explain the long-lasting contact zone of modern humans and Neanderthals. *Nat. Commun.* **10**, 5003 (2019).
135. Goni, M. F. S. Regional impacts of climate change and its relevance to human evolution. *Evol. Hum. Sci.* **2**, e55 (2020).
136. d'Errico, F. & Banks, W. E. Identifying mechanisms behind Middle Paleolithic and Middle Stone Age cultural trajectories. *Curr. Anthropol.* **54**, S371–S387 (2013).
137. Yang, S. X. et al. Technological innovations at the onset of the Mid-Pleistocene climate transition in high-latitude East Asia. *Natl Sci. Rev.* **8**, nwaa053 (2021).
138. Guan, Y. et al. Microblade remains from the Xishahe site, North China and their implications for the origin of microblade technology in Northeast Asia. *Quat. Int.* **535**, 38–47 (2020).
139. Gosling, W. D., Scerri, E. M. L. & Kaboth-Bahr, S. The climate and vegetation backdrop to hominin evolution in Africa. *Phil. Trans. R. Soc. B* **377**, 20200483 (2022).
140. d'Errico, F. et al. Identifying early modern human ecological niche expansions and associated cultural dynamics in the South African Middle Stone Age. *Proc. Natl Acad. Sci. USA* **114**, 7869–7876 (2017).
141. Ziegler, M. et al. Development of Middle Stone Age innovation linked to rapid climate change. *Nat. Commun.* **4**, 1905 (2013).
142. Moncel, M. H. et al. The origin of early Acheulean expansion in Europe 700 ka ago: new findings at Notarchirico (Italy). *Sci. Rep.* **10**, 13802 (2020).
143. Banks, W. E. et al. An application of hierarchical Bayesian modeling to better constrain the chronologies of Upper Paleolithic archaeological cultures in France between ca. 32,000–21,000 calibrated years before present. *Quat. Sci. Rev.* **220**, 188–214 (2019).
144. Gowlett, J. A. J., Harris, J. W. K., Walton, D. & Wood, B. A. Early archaeological sites, hominid remains and traces of fire from Chesowanja, Kenya. *Nature* **294**, 125–129 (1981).
145. Barbetti, M. Traces of fire in the archaeological record, before one million years ago? *J. Hum. Evol.* **15**, 771–781 (1986).
146. Zohar, I. et al. Evidence for the cooking of fish 780,000 years ago at Gesher Benot Ya'aqov, Israel. *Nat. Ecol. Evol.* **6**, 2016–2028 (2022).
147. Gowlett, J. A. J. The discovery of fire by humans: a long and convoluted process. *Philos. Trans. R. Soc. B* **371**, 20150164 (2016).
148. Wrangham, R. Control of fire in the Paleolithic: evaluating the cooking hypothesis. *Curr. Anthropol.* **58**, S303–S313 (2017).
149. Hoare, S. Assessing the function of Palaeolithic hearths: experiments on intensity of luminosity and radiative heat outputs from different fuel sources. *J. Paleol. Archaeol.* **3**, 537–565 (2020).
150. Roebroeks, W. & Villa, P. On the earliest evidence for habitual use of fire in Europe. *Proc. Natl Acad. Sci. USA* **108**, 5209–5214 (2011).
151. Hosfield, R. Walking in a Winter Wonderland? Strategies for early and middle Pleistocene survival in midlatitude Europe. *Curr. Anthropol.* **57**, 653–682 (2016).
152. Collard, M., Tarle, L., Sandgathe, D. & Allan, A. Faunal evidence for a difference in clothing use between Neanderthals and early modern humans in Europe. *J. Anthropol. Archaeol.* **44**, 235–246 (2016).
153. Carbonell, E. et al. The TD6 level lithic industry from Gran Dolina, Atapuerca (Burgos, Spain): production and use. *J. Hum. Evol.* **37**, 653–693 (1999).
154. Henshilwood, C. S., d'Errico, F., Marean, C. W., Milo, R. G. & Yates, R. An early bone tool industry from the Middle Stone Age at Blombos Cave, South Africa: implications for the origins of modern human behaviour, symbolism and language. *J. Hum. Evol.* **41**, 631–678 (2001).
155. d'Errico, F. The invisible frontier. A multiple species model for the origin of behavioral modernity. *Evol. Anthropol.* **12**, 188–202 (2003).
156. Gilligan, I. The prehistoric development of clothing: archaeological implications of a thermal model. *J. Archaeol. Method Theory.* **17**, 15–80 (2010).
157. Barham, L. et al. Evidence for the earliest structural use of wood at least 476,000 years ago. *Nature* **622**, 107–111 (2023).
158. Rodríguez, J. & Willmes Mateos, C. A. Shivering in the Pleistocene. Human adaptations to cold exposure in Western Europe from MIS 14 to MIS 11. *J. Hum. Evol.* **153**, 102966l (2021).
159. Castiglione, S. et al. A new method for testing evolutionary rate variation and shifts in phenotypic evolution. *Methods Ecol. Evol.* **9**, 974–983 (2018).
160. Banks, W. E., d'Errico, F. & Zilhao, J. Human-climate interaction during the Early Upper Paleolithic: testing the hypothesis of an adaptive shift between the Proto-Aurignacian and the early Aurignacian. *J. Hum. Evol.* **64**, 39–55 (2013).
161. Esteban, I., Albert, R. M., Eixea, A., Zilhao, J. & Villaverde, V. Neanderthal use of plants and past vegetation reconstruction at the Middle Paleolithic site of Abrigo de la Quebrada (Chelva, Valencia, Spain). *Archaeol. Anthropol. Sci.* **9**, 265–278 (2017).
162. Oppenheimer, S. The great arc of dispersal of modern humans: Africa to Australia. *Quat. Int.* **202**, 2–13 (2009).
163. Rasheed, S. M. & Billingham, J. A. Reaction diffusion model for inter-species competition and intra-species cooperation. *Math. Model. Nat. Phenom.* **8**, 154–181 (2013).
164. Alroy, J. A multispecies overkill simulation of the end-Pleistocene megafaunal mass extinction. *Science* **292**, 1893–1896 (2001).
165. Wakano, J. Y., Gilpin, W., Kadowaki, S., Feldman, M. W. & Aoki, K. Ecocultural range-expansion scenarios for the replacement or assimilation of Neanderthals by modern humans. *Theor. Pop. Biol.* **119**, 3–14 (2018).
166. Flores, J. C. A mathematical model for Neanderthal extinction. *J. Theor. Biol.* **191**, 295–298 (1998).
167. Gilpin, W., Feldman & Aoki, K. An ecocultural model predicts Neanderthal extinction through competition with modern humans. *Proc. Natl Acad. Sci. USA* **113**, 2134–2139 (2016).
168. Manna, K., Volpert, V. & Banerjee, M. Pattern formation in a three-species cyclic competition model. *Bull. Math. Biol.* **83**, 52 (2021).
169. Neuhauser, C. & Pacala, S. W. An explicitly spatial version of the Lotka-Volterra model with interspecific competition. *Ann. Appl. Probab.* **9**, 1226–1259 (1999).
170. Okubo, A., Maini, P. K., Williamson, M. H. & Murray, J. D. On the spatial spread of the grey squirrel in Britain. *Proc. R. Soc. B* **238**, 113–125 (1989).
171. Young, D. A. & Bettinger, R. L. The numic spread: a computer simulation. *Am. Antiq.* **57**, 85–99 (1992).
172. Timmermann, A., Wasay, A. & Raia, P. Phase synchronization between culture and climate forcing. *Proc. R. Soc. B* **291**, 20240320 (2024).
173. Einstein, A. Über die von der molekularkinetischen Theorie der Wärme geforderte Bewegung von in ruhenden Flüssigkeiten suspendierten Teilchen. *Ann. Phys.* **322**, 549–560 (1905).
174. Hasselmann, K. Stochastic climate models. 1. Theory. *Tellus* **28**, 473–485 (1976).
175. Powell, A., Shennan, S. & Thomas, M. G. Late Pleistocene demography and the appearance of modern human behavior. *Science* **324**, 1298–1301 (2009).
176. Henrich, J. Demography and cultural evolution: how adaptive cultural processes can produce maladaptive losses — the Tasmanian case. *Am. Antiq.* **69**, 197–214 (2004).
177. Aoki, K. Gene-culture waves of advance. *J. Math. Biol.* **25**, 453–464 (1987).
178. Bergström, A., Stringer, C., Hajdinjak, M., Scerri, E. M. L. & Skoglund, P. Origins of modern human ancestry. *Nature* **590**, 229–237 (2021).
179. Petr, M., Paabo, S., Kelso, J. & Vernot, B. Limits of long-term selection against Neandertal introgression. *Proc. Natl Acad. Sci. USA* **116**, 1639–1644 (2019).
180. Zhang, X. J. et al. The history and evolution of the Denisovan-EPAS1 haplotype in Tibetans. *Proc. Natl Acad. Sci. USA* **118**, e2020803118 (2021).
181. Huerta-Sanchez, E. et al. Altitude adaptation in Tibetans caused by introgression of Denisovan-like DNA. *Nature* **512**, 194–197 (2014).

182. Vespasiani, D. M. et al. Denisovan introgression has shaped the immune system of present-day Papuans. *PLoS Genet.* **18**, e1010470 (2022).
183. Currat, M., Ray, N. & Excoffier, L. SPLATCHE: a program to simulate genetic diversity taking into account environmental heterogeneity. *Mol. Ecol. Notes* **4**, 139–142 (2004).
184. Douka, K. et al. Age estimates for hominin fossils and the onset of the Upper Palaeolithic at Denisova Cave. *Nature* **565**, 640–644 (2019).
185. Jacobs, G. S. et al. Multiple deeply divergent Denisovan ancestries in Papuans. *Cell* **177**, 1010–1021 (2019).
186. Larena, M. et al. Philippine Ayta possess the highest level of Denisovan ancestry in the world. *Curr. Biol.* **31**, 4219–4230 (2021).
187. Liu, H., Prugnolle, F., Manica, A. & Balloux, F. A geographically explicit genetic model of worldwide human-settlement history. *Am. J. Hum. Gen.* **79**, 230–237 (2006).
188. Tebaldi, C. & Knutti, R. The use of the multi-model ensemble in probabilistic climate projections. *Phil. Trans. R. Soc. A* **365**, 2053–2075 (2007).
189. Steffen, W. et al. Trajectories of the Earth system in the Anthropocene. *Proc. Natl Acad. Sci. USA* **115**, 8252–8259 (2018).
190. Thornley, J. H. M. & France, J. An open-ended logistic-based growth function. *Ecol. Model.* **184**, 257–261 (2005).
191. Rockström, J. et al. Safe and just Earth system boundaries. *Nature* **619**, 102–111 (2023).
192. Andersen, K. et al. High-resolution record of Northern Hemisphere climate extending into the last interglacial period. *Nature* **431**, 147–151 (2004).
193. Kaplan, J. O. M. New, Arctic climate change with a 2 °C global warming: timing, climate patterns and vegetation change. *Clim. Change* **79**, 213–241 (2006).
194. Chan, E. K. F. et al. Human origins in a southern African palaeo-wetland and first migrations. *Nature* **575**, 185–189 (2019).
195. Schlebusch, C. M. et al. Southern African ancient genomes estimate modern human divergence to 350,000 to 260,000 years ago. *Science* **358**, 652–655 (2017).

Acknowledgements
A.T., K.-S.Y. and E.Z. received funding from the Institute for Basic Science (IBS) under IBS-R028-D1.

Author contributions
A.T. and P.R. conceived and organized the text and led the writing. M.P.deL. and C.Z. provided key contributions to the ABM and cultural evolution sections. A.M. provided key contribution to the SDM section. K.-S.Y. and E.Z. provided key contributions to the description of palaeoclimate and vegetation modelling. All authors critically reviewed the text and participated in writing.

Competing interests
The authors declare no competing interests.

Additional information
Peer review information *Nature Reviews Earth & Environment* thanks Ariane Burke, William Banks and the other, anonymous, reviewer(s) for their contribution to the peer review of this work.

Publisher's note Springer Nature remains neutral with regard to jurisdictional claims in published maps and institutional affiliations.